Master's Thesis

GENERATION OF LOAD-SPECIFIC LATTICE STRUCTURE USING TOPOLOGY OPTIMIZATION OF BUILDING BLOCKS FOR ADDITIVE MANUFACTURING

Haejoon Choi

Department of System Design and Control Engineering

Graduate School of UNIST

2019

Master's Thesis

Generation of Load-specific Lattice Structure Using Topology Optimization of Building Blocks for Additive Manufacturing

Haejoon Choi

Department of System Design and Control Engineering

Graduate School of UNIST

Generation of Load-specific Lattice Structure Using Topology Optimization of Building Blocks for Additive Manufacturing

A thesis
submitted to the Graduate School of UNIST
in partial fulfillment of the
requirements for the degree of
Master of Science

Haejoon Choi

12/10/2018 of submission

Approved by

Namhum Kim

Advisor
Namhum Kim

Generation of Load-specific Lattice Structure Using Topology Optimization of Building Blocks for Additive Manufacturing

Haejoon Choi

This certifies that the thesis of Haejoon Choi is approved.

12/10/2018 of submission

Advisor: Namhun Kim

Duck Young Kim

Juhwan Oh

Abstract

One of the design theories and methodologies, design for additive manufacturing (DFAM) has great importance in making additive manufacturing (AM) feasible to the industry. DFAM can be used to add new features, make sturdier and lighter structure, and streamline the design and manufacturing process of AM. As AM is not currently applicable to every sector in the industry, it is best to take full advantages of AM.

However, DFAM methods including topology optimization (TO) cannot be implemented directly to AM. Even though AM is well-known for its design freedom and ability to fabricate complex structures, limiting factors like overhang regions in the structure demand support structures to prevent manufacturing failures such as sagging. As support structure requires additional design steps and its removal after the fabrication, meaning a longer process time, cost and poor surface finish, general users of AM face difficulties in processing.

In this work, a lattice structure generation method is presented to ease the implementation of DFAM concepts to the AM part design. “Building Blocks” are generated by applying TO to unit cells with various stress conditions which later are stacked using MATLAB, a programming platform. The resulting lattice structures are later compared with the structures generated using conventional TO method. The presented methodology shows significant reduction of the elapsed time for the structure generation. This method is remarkable in that, as it does not require a deep understanding and knowledge of FEA and TO, it is easily accessible to the general public.

Contents

List of Figures

List of Tables

List of Equations

1. Introduction

1.1 Background

Additive Manufacturing refers to the manufacturing technologies that fabricates parts by adding up material to the substrate in a layer-by-layer fashion [1]. Compared to the conventional subtractive that works by removing layers of work material using machine tools, AM has advantages on reducing material wastage, energy consumption, and harmful chemicals in manufacturing, and on streamlining the design process [2-4].

In most cases, AM technology was used as a mean of rapid prototyping during the product development stage. Due to inferior size accuracy, mechanical properties and limitation of material types, AM was not considered satisfactory to produce final parts. However, with recent improvements of AM machines, developments of materials and implementation of design for additive manufacturing (DFAM), 3D printed products are now more accepted as end-products [3, 5].

Stated in the Wohler Report 2018, an estimated $918.6 million was spent on final part manufacturing using AM, and this is rapidly increasing each year as illustrated in Figure 1.1. In 2017, the percentage of the growth was 32.4% [6]. Still, the estimated money spent on final part production holds for only 12.5% of the total revenue. AM is yet to be mainly utilized to manufacture final parts.

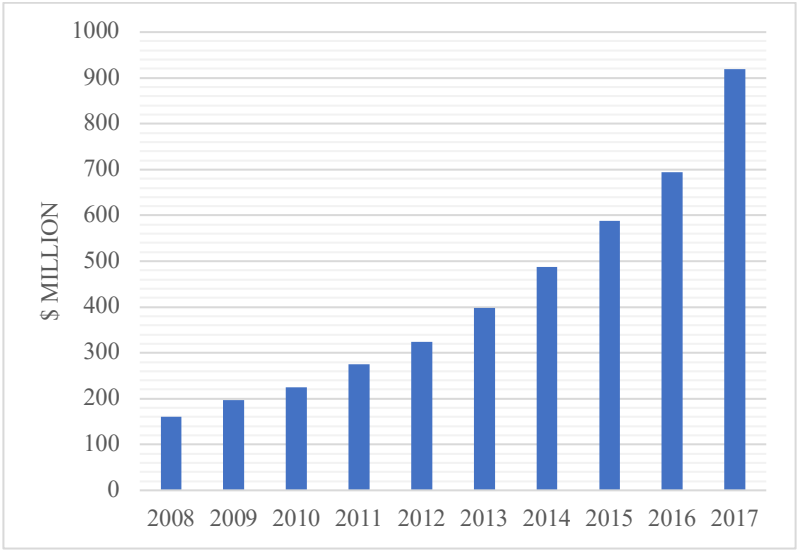

Figure 1.1 The Estimated Money Spent on Final Part Production using AM [6]

Additive manufacturing is preferable when it is applied on small, intricate parts in small quantity [7]. In order to fully maximize the benefits of AM and obtain economic feasibility that the industry demands, the application of design for additive manufacturing (DFAM) is indispensable [8]. DFAM was developed because parts designed with conventional design methodology is not appropriate when it is manufactured with AM; parts explicitly designed for AM through DFAM showed the high possibility of improvements [9].

Among the DFAM methods, topology optimization (TO) and lattice structure design (also called, periodic cellular structure) are commonly used by researchers to improve the performance of the structure or add user-defined features [10-12].

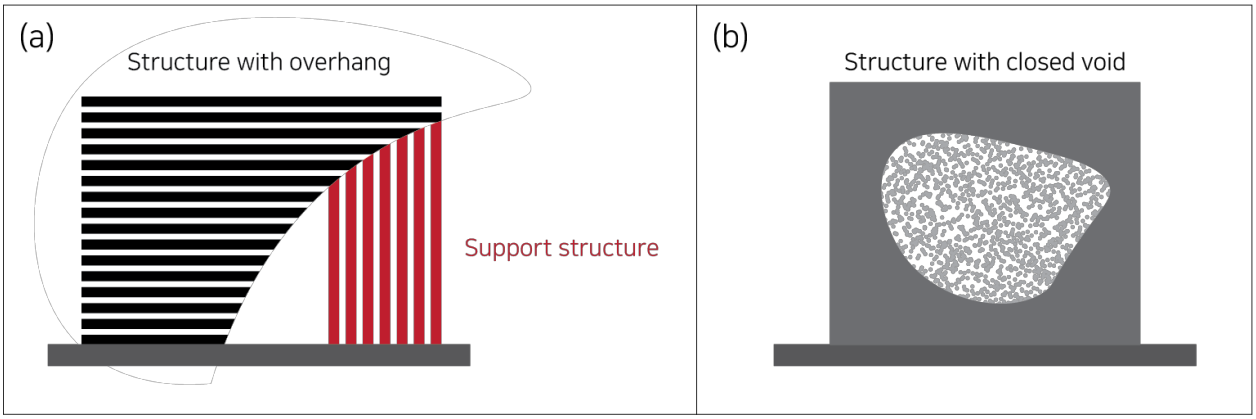

Figure 1.2 Obstacles in the Fabrication of Complex Structures using AM

Topology optimization is an optimization method that finds optimal topology out of given design space by minimizing defined objective function such as compliance, fundamental natural frequency or electromagnetic properties. Along with the lattice structures, the resulting structures from TO method often have complex shapes that are quite difficult to process through conventional manufacturing method. One advantage of AM is capability of fabricating such complex and superior structures.

Still, there are some obstacles even when fabricating complex structures with AM. For instance, the fabrication of overhang structure requires support structure, except when using selective laser sintering method, as shown in Figure 1.2 (a). Support structures should be carefully placed as they affect the fabrication time, cost, and its removal process. In the case of the powder bed fusion method, closed void should be avoided as excess material can be trapped inside as illustrated in Figure 1.2 (b). Even though many cases showing improvements made with AM exist, many companies are still not adopting DFAM methods in the manufacturing of final parts. It can be one of the reasons why AM is only confined in very narrow industry sectors where long and customized design process is tolerable such as medical, dental and aerospace industries.

1.2 Objectives

The objective is to develop a simple structure generation method that can help AM users build a periodic structure that has written advantages of the TO and lattice structure but doesn't create problems related to the details of the additive manufacturing process.

To achieve the described attributes, various pre-optimized unit cells were introduced as "Building Blocks," and a library for these blocks was generated. As building blocks are generated through TO process, the performance and manufacturability of each block can be guaranteed.

In order to create a structure that is customized to each mechanical design problem, the structural analysis data obtained from FEA analysis on the design space was employed. Stress distribution of the design space was analyzed and used for the building blocks stacking process. As FEA analysis is computationally lighter than TO and analysis of the stress distribution is relatively simple, the processing time for the generation of lattice structure can be significantly reduced.

1.3 Outline

In Chapter 2, related researches to the topic of the thesis were reviewed. Studies on DFAM, topology optimization for AM and the feasibility of AM were covered. Also, an application of DFAM to the production of an electric bicycle was presented to show the practical design and manufacturing process of AM.

In Chapter 3, the developed method to generate lattice structures with pre-optimized building blocks is presented. The description of the presented method and a comparison between the design space, the structure made with TO, and the structures made with the suggested method are given.

2. Background

2.1 Feasibility of Additive Manufacturing

Showing great potential, additive manufacturing (AM) has drawn exceptional attention of the public. However, as discussed previously, AM is not being used as a major method of manufacturing final parts in the industry. There are some studies which let us understand why AM is only suitable for some sections of the industry and not for others. By examining these researches, we will be able to understand how we could wisely use the AM technology to the final part production.

Conner et al. [7] developed a reference system (Figure 2.1) to assess the levels of volume, customization, and complexity of manufactured products, as the factors are assumed to be crucial when choosing between conventional and additive manufacturing for the production. Products could be categorized into eight regions in the reference system by their levels of volume, complexity, and customization. They also developed a method of determining the levels of complexity and customization of products. With the reference system and method of determining the levels of complexity and customization, they examined the competitive advantages of AM compared to conventional manufacturing methods. Case studies revealed that products that fall into the region ③ to ⑧ potentially have a competitive advantage to the conventional manufacturing and further analysis would be needed to determine the production method. For the products that falls into the region ②, can have a competitive advantage only if AM can produce them at lower cost or shorter lead time.

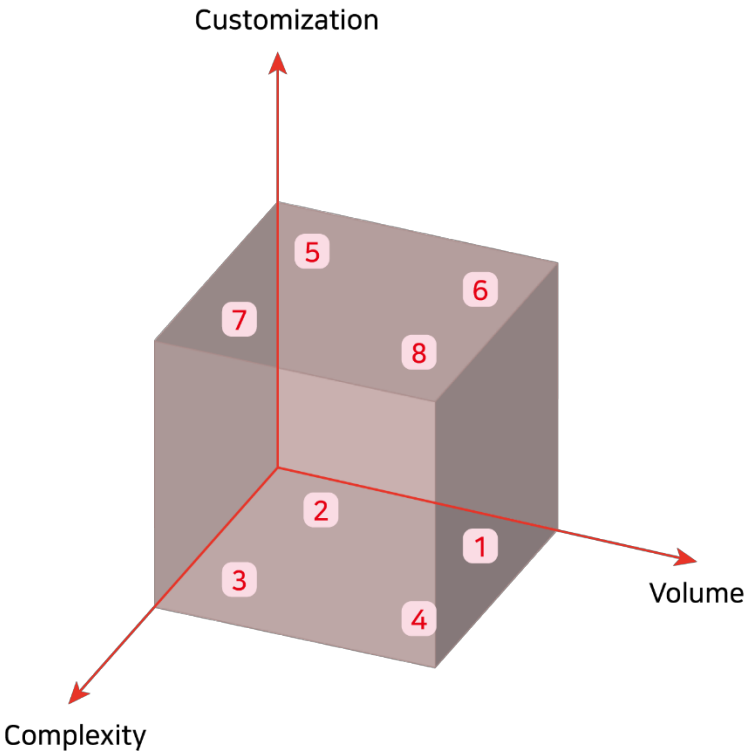

1	Mass Manufacturing
2	Manufacturing of the Few
3	Complexity Advantage
4	Mass Complexity
5	Customized for the Individual
6	Mass Customization
7	Artisan Products
8	Complete Manufacturing Freedom

Figure 2.1 Reference System (Conner et al. [7])

Atzeni et al. [13] demonstrated economic feasibility of the AM process compared to High-Pressure Die Casting (HPDC) process. Cost evaluation models of HPDC and AM processes were developed and production of the landing gear of a 1:5 scaled model aircraft as analyzed. For the analysis, the landing gear was redesigned to utilize the advantages of the AM process and validated with ABAQUS finite element analysis. Cost per assembly with an increasing number of production volume showed that AM has a competitive advantage in cost under 42 pieces of production volume. As HPDC requires an expensive mold production cost, but it is diluted as production volume increases, the cost per assembly decreases as production volume grows.

2.2 Design for Additive Manufacturing

Design for additive manufacturing (DFAM) is one of the categories in Design Theory and Methodology (DTM), it provides the theoretical background to design a product well. One of the DTM theories, Design for X (DFX) refers to design theories that have objective as X-factor in the design. As AM has significant differences with conventional manufacturing methods, Design for Additive Manufacturing was developed to maximize the advantages of AM process.

Yang et al. represented that AM influenced the design theory and methodology (DTM) as it alleviated shape complexity constraints of conventional manufacturing [8]. They reviewed the

influence of AM on conventional Design Theory and Methodology (DTM). Three different DFX theories which are Design for Manufacturing (DFM), for Assembly (DFA), and Performance (DFP) were analyzed. The authors analyzed the challenges of previous DFX theory caused by attributes of AM as AM enables design freedom, parts can be designed and modules and combined later, material composition can be varied in the structure domain, hierarchical complexity can be achieved, remanufacturing or repairing are enabled, parts integration can be done quickly, joining different parts can be done. As conventional DTM cannot take full advantage of AM technology, DFAM was developed.

The authors claim that there are generally two categories of DFAM, one with a focus on structural optimization method for AM-enabled design and the other with methodologies of DFAM. Generally, the structural optimization for the different objectives can be conducted with topology optimization (TO) method. Many researchers focus on the TO for making a structure with superior characteristics that were unable to achieve with conventional manufacturing or generating better lattice structure by varying structure parameters. Methodologies of DFAM includes the entire process of AM such as requirements of the product, redesign or parts integration, structural or shape optimization, determination of AM process and parameters and orientation of parts inside the build volume [14].

The authors proposed the DFAM method which consists of design specifications, design processes, and process constraints. In the first step of the method, functional integration of parts from the initial CAD model is conducted. This means a designer would consolidate several parts with the same functional purposes into one. In the second step, optimization of the structures that are integrated is done. This optimization can be either TO or application of hierarchical structure such as lattice structure. The purpose of the optimization can be achieving lighter weight, stiffer structure, dynamic properties or better heat dissipation. The last step of the method is about the iteration. If a design solution is created, then the design process is done, else, the design flow should be repeated from the first step again.

Ponche et al. studied the global approach of DFAM [14]. Comparing with the partial approach of DFAM which starts from initial CAD design that is generally designed bearing conventional manufacturing in mind, the authors suggested global design approach that a designer starts with constraints or requirements of the part design considering AM as a mean of manufacturing. A new global DFAM methodology was suggested with a case study was conducted on a redesign of the robotic system.

2.3 Topology Optimization (TO) for DFAM

Studies related to the use of TO for DFAM can be categorized into 2 kinds of topics. The first is the studies that apply TO for DFAM so that it adds a new attribute to parts that were impossible or very difficult to be achieved. The second is the studies that change the methodology or process of TO in order to apply it to DFAM more effectively.

Among the first category studies, Andreassen et al. (Figure 2.2.a) utilized TO to generate negative Poisson's ratio structure and AM to fabricate a delicate complex structure that is generally impossible to be built with conventional manufacturing methods [12]. Formulation of Poisson's ratio minimization problem was developed, and minimum Poisson's ratio topology for 2D and 3D were driven. Fabricating such complex structure showed the possibility of AM applications.

Moon et al. (Figure 2.2.b, Figure 2.2.c) applied TO concept to fabrication of unmanned aerial vehicle [15]. In order to achieve light-weight and sturdy structure for the wing structure, the authors generated three different cellular structures and evaluated the response of the wings under compressive load testing.

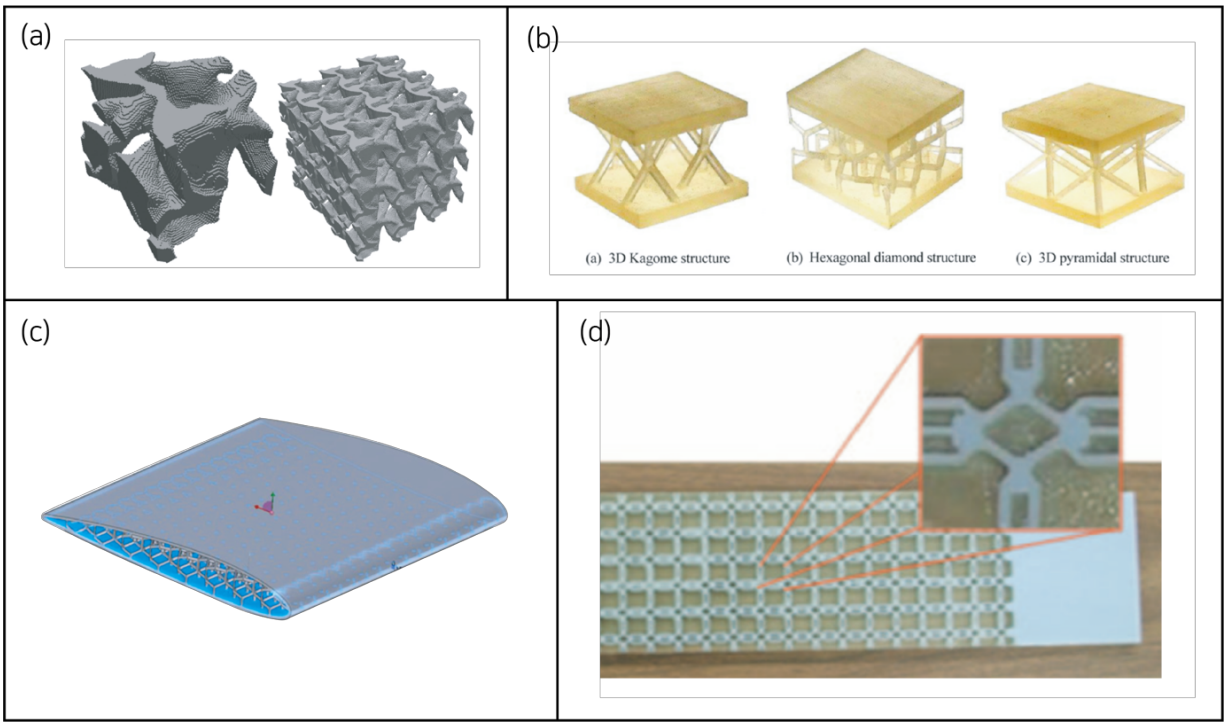

Figure 2.2 (a) Andreassen et al. [12] (b, c) Moon et al. [15] (d) Joo et al. [16]

Joo et al. (Figure 2.2.d) developed a 2-step method to determine the structure of aircraft flexible wing skin. Among aircraft, there are some models with sweep wings that can change the wing shape while the aircraft flies [16]. It has benefits that the optimal sweep angle is different between high-speed and low-speed running condition. Generally, low sweep angle has benefits at low-speed,

fuel efficient running condition and the high-sweep angle is better at the high-speed condition that needs low drag force on the body of aircraft. In order to realize the flexible wing that can be swept, the heterogeneous mechanical property is needed for the skin of the wing. In order to realize this, the authors implemented a 2-step optimization that first, they optimize the bulk material properties to get the desired shape when the wing is deformed, and second, to obtain the optimal material allocation, homogenization method was used to get the desired mechanical properties with periodic microstructure. Using AM, they fabricated the periodic structure and validated the mechanical property.

Bickel et al. studied the fabrication of shoe inserts with a similar approach [17]. They made a library of non-linear mechanical properties on base materials for the insert and optimization process was implemented to derive the optimum combination of the materials. The different resulting stiffness of the inserts could be generated using the optimization process.

Lin et al. utilized TO and AM for the medical application [18]. Lumbar interbody fusion cage can be used for the spinal arthrodesis for the patients who have pathological spinal disorders. These cages have generally been produced using porous tantalum structure because the cage should have excellent biocompatibility, permeability and similar mechanical properties with bones since the permeability and mechanical property have a direct influence on the healing process of adjacent bones.

Selective laser melting (SLM) process which is one of powder bed fusion AM methods can be used to fabricate the parts with titanium alloy that has good biocompatibility. Using SLM process with TO that enabled the generation of the structure with specific stiffness, the authors could fabricate parts with desired properties with consistency. The porous tantalum cage had issues with consistency of mechanical properties, and poor visibility on CT scanned images. However, titanium alloy cages fabricated with SLM had no issues with the inconsistency of mechanical properties, or CT scanned images.

Chen et al. also used AM and TO for the design of the bio-medical application, which is biodegradable scaffolds [19]. This structure also requires specific properties such as similar mechanical properties with adjacent tissues, good permeability for the nutrients transportation, and controlled degradation rate. In order to obtain the optimal scaffold design, the authors implemented a multi-objective optimization process that has permeability and stiffness functions with weights as objectives. Various scaffolds could be derived using different weights for the objective functions. Degradation process model of the scaffold structure could be derived, and simulation of the healing process in the tissue was conducted.

Castilho also used TO and AM for fabrication of bone tissue engineering. For the treatment of cruciate ligament rupture in dogs, tibial tuberosity which is a process linking two bones is known

for its stabilizing effect on the bones. Calcium phosphate scaffold could be used for this occasion, and 3DP process with sintering was considered optimal for the fabrication process. The authors implemented TO to maximize the permeability of the structure while constraining the stiffness to the level of bones. They could fabricate the scaffold model using the 3DP process and validate the performance of the structure.

The second category of TO-related DFAM studies that change the methodology or process of TO to generate the structure more effectively includes studies below.

Wang et al. (Figure 2.3.a) developed concurrent TO method to integrate the macro and micro TO into one algorithm [11]. In order to generate a TO derived structure constructed with micro-scale cell structures, the authors parameterized cell structures with a variable and derived interpolated model of effective stiffness matrix of the cell structures. By setting objective variables as density value and the cell structure parameter of each cell, the optimization problem could solve macro and micro TO problem concurrently. With several assumptions on the problem and the help of pre-derived effective stiffness matrix of the parameterized cell structures, derivative of the optimization problem could be derived analytically. Thus, the TO problem could be solved with gradient-based optimization solver, in this case, globally convergent version of the method of moving asymptotes was used. Resulting structure had non-uniform lattice microstructure, and the macrostructure was also topologically optimized. The structure showed better stiffness than compared structures.

Gorguluarslan et al. (Figure 2.3.b) suggested a new 2-phase framework to optimize the lattice structure [20]. The authors first generated a lattice structure with several pre-determined structures such as OctetFramed, Cross or Octet and the first optimization process with strut diameters as design variables. Resulting lattice structures included struts with near-zero diameter. Thus, struts with diameters under pre-determined value were deleted because they cannot be fabricated with the AM method. Second optimization phase included minimum strut size constraint so that the resulting structure would be feasible for the AM process. The 2-phase TO process was claimed to be efficient because the first phase of the process does not require the minimum strut size constraint that can significantly raise the computation time. The second phase of the optimization is conducted only for the remaining struts after deletion of infeasible struts so that the computation amount could be reduced.

Ma et al. (Figure 2.3.c) suggested multi-domain multi-step topology optimization (MMTO) approach [21]. The authors developed a multi-domain topology optimization (MDTO) method that is a TO method that sequentially solves TO problems in multi-domains possibly with different material for each domain. Also, multi-step topology optimization (MSTO) was defined as a TO method that initial TO problem is solved with comparatively rough mesh and the resulting structure is filtered, and then successive optimizations with finer mesh are solved. The authors defined

MMTO as a combination of MDTO and MSTO. The authors could generate a structure by solving the MMTO problem with minimization of dynamic response. Validation of the generated structure was conducted virtually and physically.

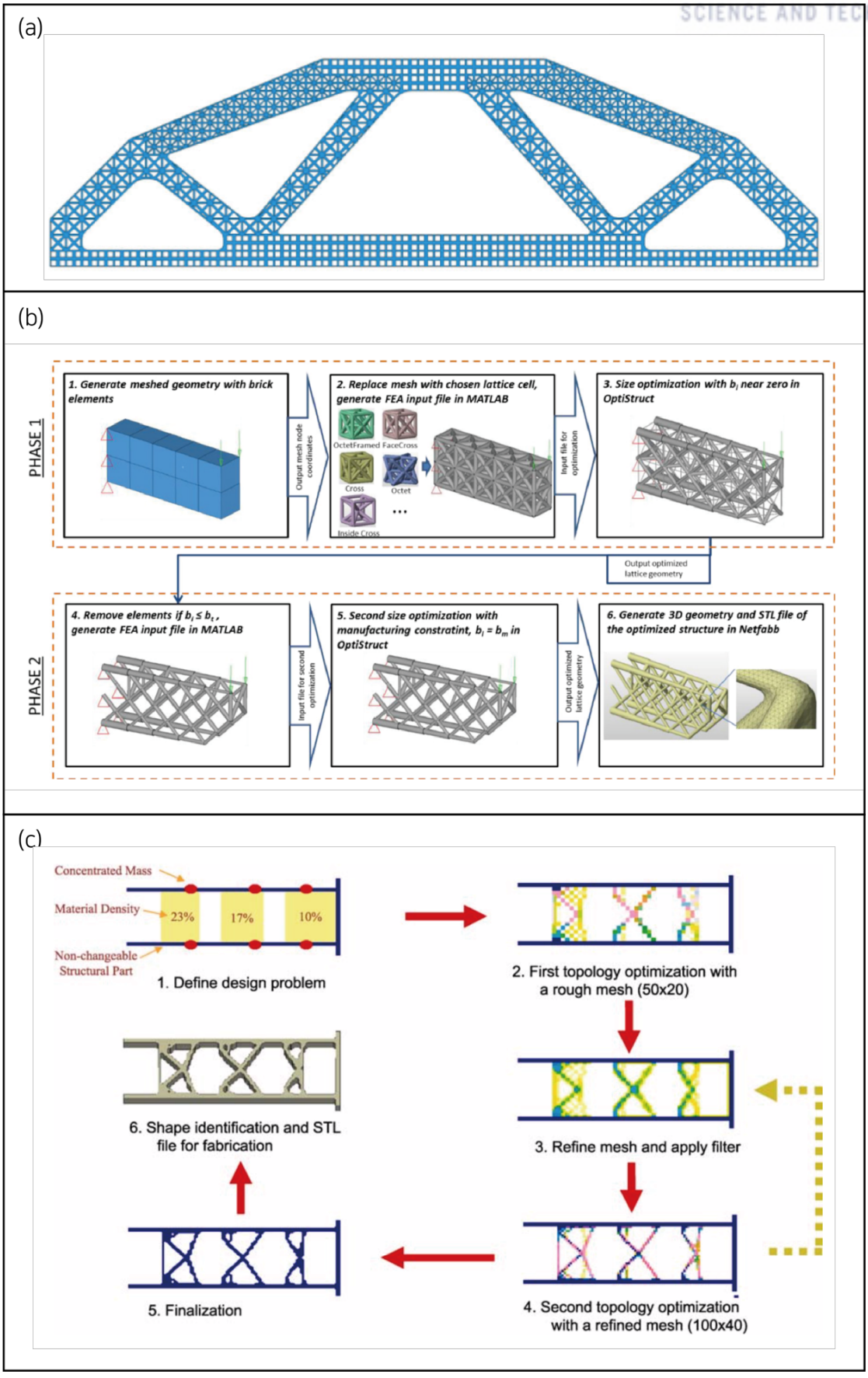

Figure 2.3 (a) Wang et al. [22] (b) Gorguluarslan et al. [20] (c) Ma et al. [21]

2.4 Example of DFAM – Case Study

2.4.1 Application of DFAM: Design of Electric Bicycle Frame

In this section, design for additive manufacturing (DFAM) including topology optimization (TO) was conducted to design an electric bicycle frame using additive manufacturing (AM). There ar e many applications of AM to the productions of specialized parts for bio-medical, aerospace and automotive industries, but they are mostly confined to the fabrication of a particular part of the assembly without any comparison of building time and cost. The case study conducted here shows the possibility of applying AM process to the every-day product, which in this case is the electric bicycle.

2.4.2 An Overview of AM Process with DFAM

- **The Difference Compared to the Conventional Manufacturing Process**

With DFAM, which enables new features and high efficiency on the production of additively manufactured parts, the steps of the manufacturing process are different with the conventional manufacturing process. In the conventional manufacturing process, the design of a product starts with the mechanical design by an engineer. The designer considers the constraints and objectives of the part, based on his or her mechanical design knowledge. Then, the needed material, thickness or length of parts of the product are calculated. The preliminary design is produced as a prototype and goes through an assessment process that could be physical or virtual. Then, the part is redesigned according to the assessment of the part. The entire process for the traditional design process takes a long time because not only the part design needs to be designed manually, but also prototyping & validation of the part also take some time.

In AM with DFAM method, the design process is different from the conventional design process. In the DFAM design process, with the constraints and requirements of a part, the design space is designated, and TO problem is generated with user-defined objective functions and constraints. By solving the TO problem, a designer derive the optimized structure and generate the preliminary design with a little post-processing through the computer-aided engineering (CAE) software. Based on the preliminary design, a designer can further modify the structure of the part to make it feasible for the actual application.

Finite element analysis (FEA) to the designed part also can be conducted to assess the performance of the part design. Using the requirements and constraints of actual application, designer can simulate the reaction of the part to the external stimuli and get meaningful data on the

performance of the structure such as effective stiffness, fundamental resonance frequency, maximum displacement or stress distribution. Considering the analysis results, a designer can choose between modification of the optimization problem and manual modification to the design. If the designer chooses the modification of the optimization problem, the process can be repeated until the satisfying structure is derived, if not, the designer can directly modify the design manually and assess the design again. This design–assessment–redesign process can be done quicker than conventional process thanks to TO and FEA. Often, it is called data-driven design process because the design of the structure is driven from the requirements and constraints of the design problem with the optimization model.

This design process suits well with the AM process because AM process significantly eases the constraints on the shape realization. In the conventional design process, the designer should exactly know the limitation of each manufacturing method on the shape realization as most TO-based designs contain complex geometry and unreachable inner structure. However, because AM can possibly fabricate virtually any complex shape, designer can concentrate on the performance and features of the parts.

- **Topology Optimization**

TO is one of the optimization algorithms to get the optimum structure (topology) by minimizing an objective function subject to equal or unequal constraints. The TO problem can be expressed mathematically as below.

$$\begin{aligned} &\text{Minimize} \quad C(\rho_i) = \boldsymbol{F}^T\boldsymbol{U} = \boldsymbol{U}^T\boldsymbol{K}\boldsymbol{U} \ ; \\ &\text{subject to} \quad \boldsymbol{K}\boldsymbol{U} = \boldsymbol{F} \\ &\qquad\qquad V = \sum \rho_i v_i \le \overline{V}, \\ &\qquad \text{where} \ \ \eta \le \rho_i \le 1, i = 1, \dots, n \end{aligned} \qquad \textbf{Equation 2.1}$$

In Equation 2.1 the subjective function $C(\rho_i)$ means the compliance that is expressed in strain energy. **U** is displacement vectors in nodes and **F** is force vectors. $\overline{V}$ is an objective volume that user wants to achieve, ρ_i and v_i represents the density and volume value of each element. Constant η is a small number to avoid the singularity of the calculation. Along with the global stiffness matrix **K,** the **KU=F** represents the governing equation of the entire structure. As $\mathbf{F^TU}$ represents strain energy compliance minimization problem is equivalent to the strain energy minimization and it actually minimizes the displacement vectors in each node [23]. Thus, TO process is an optimization method that solves for the density values in each element and resulting densities have values between 0 and 1. In a real situation, there is no such density value between 0 and 1. In order

to deal with this problem, the penalization method were developed to disadvantage the values between 0 and 1 so that density values converges to decimal number 0 or 1 . The software used for TO process in this chapter uses a solid isotropic material with penalization (SIMP) method to get a definite structure [24].

The actual TO and design process of the bicycle was conducted using solidThinking Inspire® 2016. Several TOs were done to efficiently obtain the optimum structure for the bicycle frame design and post-processing the rugged design derived from TO.

- **Powder Bed Fusion Technology**

In this study, one of the powder bed fusion technology, selective laser sintering (SLS) was used to produce the frame structure. Powder bed fusion technology can be defined as “an additive manufacturing process in which thermal energy selectively fuses regions of a powder bed” in ASME standard F2792 – 12a [13]. Powder bed fusion technology generally divided into three main technologies on the market namely, selective laser sintering (SLS), selective laser melting (SLM) and electron beam melting (EBM).

SLS process uses a laser beam as a source of thermal energy and sinters polymer powder to fabricate free-shape parts as illustrated in Figure 2.4.

The chamber is filled with inert gas, and the heater heats up the atmosphere to just below the melting point of the powder material before the sintering process begins. Mirror in the system rotates to direct the laser beam to the desired region that needs to be sintered. After the first layer of the part is solidified, the powder bed lowers, and powder roller spread material on top of the previous layer while rolling from the end of the powder supply to the other side passing through the powder bed. Then the sintering process using laser beam repeated until every layer is solidified. As raw powder material supports solidifying parts, there is no need for support structure and it enables the complex structure of the parts made with the SLS method.

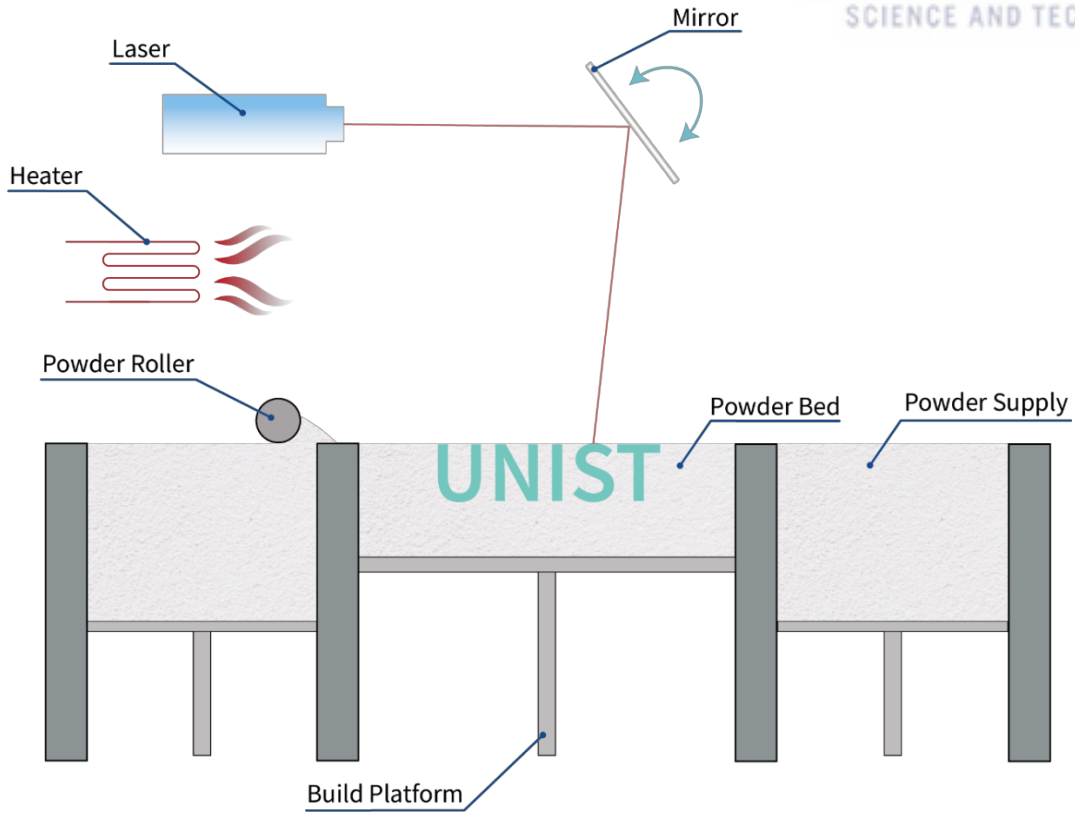

Figure 2.4 The Schematic of Powder Bed Fusion Technology

2.4.3 Design of Electric Bicycle Frame

For the TO process, setting up an optimization problem which is done by designating design space and load/support conditions in the GUI of inspire software is the first thing that must be done. It can be interpreted as setting the density variable and constraints for the optimization expression. Designation of the design space for the design of electric bicycle followed requirements described below.

First, the bicycle was planned to be 100% electric motor-driven. As users don't need to move the center of mass forward to pedal, an assumption was made for the loading condition as follows. 90% of the weight of the passenger is applied to the saddle, and the rest 10% is applied to the handlebars. Second, for the compatibility with existing common parts of the 16-inch bicycles, regions where the frame body connected to the rear wheel and the front fork were designed to be fitted with standard 16-inch ordinary bicycles. Third, the frame should be sectioned later for the SLS fabrication process because the bed volume of the SLS system was 381×330×437mm, which is smaller than the total size of the bicycle frame.

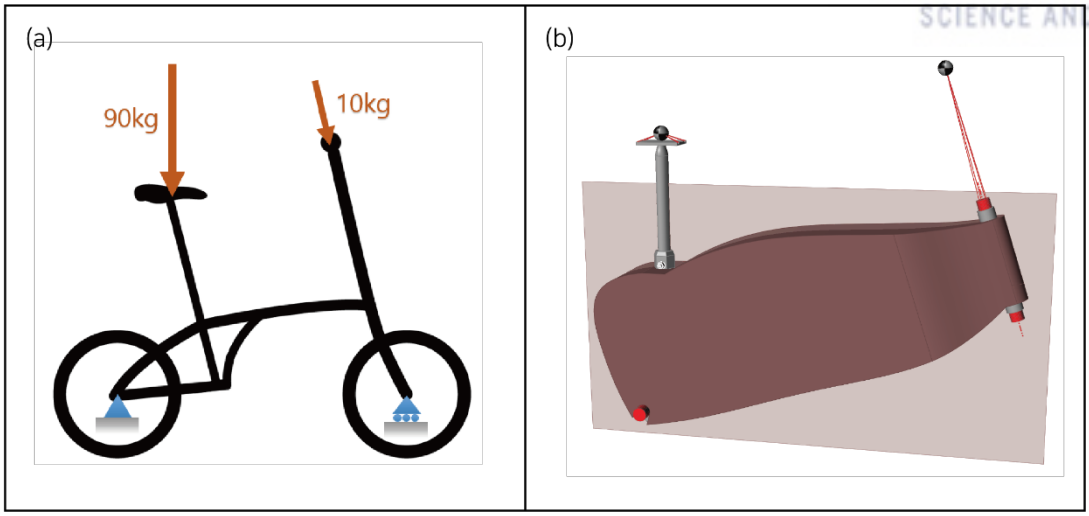

Figure 2.5 (a) Design Space for Topology Optimization (b) Loading Condition of Pedal-less Electric Bicycle

Therefore, from the first requirement, the design space and the load case for the TO could be expressed as Figure 2.5.a. The design space under the load case was generated in the Inspire® software as depicted in Figure 2.5.b. Design space is colored with reddish brown color and non-design space parts such as seat post and front fork are colored with grey. Non-design space parts are excluded from the topology optimization domain.

Figure 2.6.a shows the part after first TO and smoothing, and Figure 2.6.b shows the part was designated as design space again and topologically optimized. After smoothing the second optimization result and attaching the parts where seatpost and handle post as shown in Figure 2.6.c. Figure 2.6.d shows the part divided into three parts so that it can be printed in the SLS printer with minimal batches. A groove was made to firmly hold a battery pack in the hollow space of the frame.

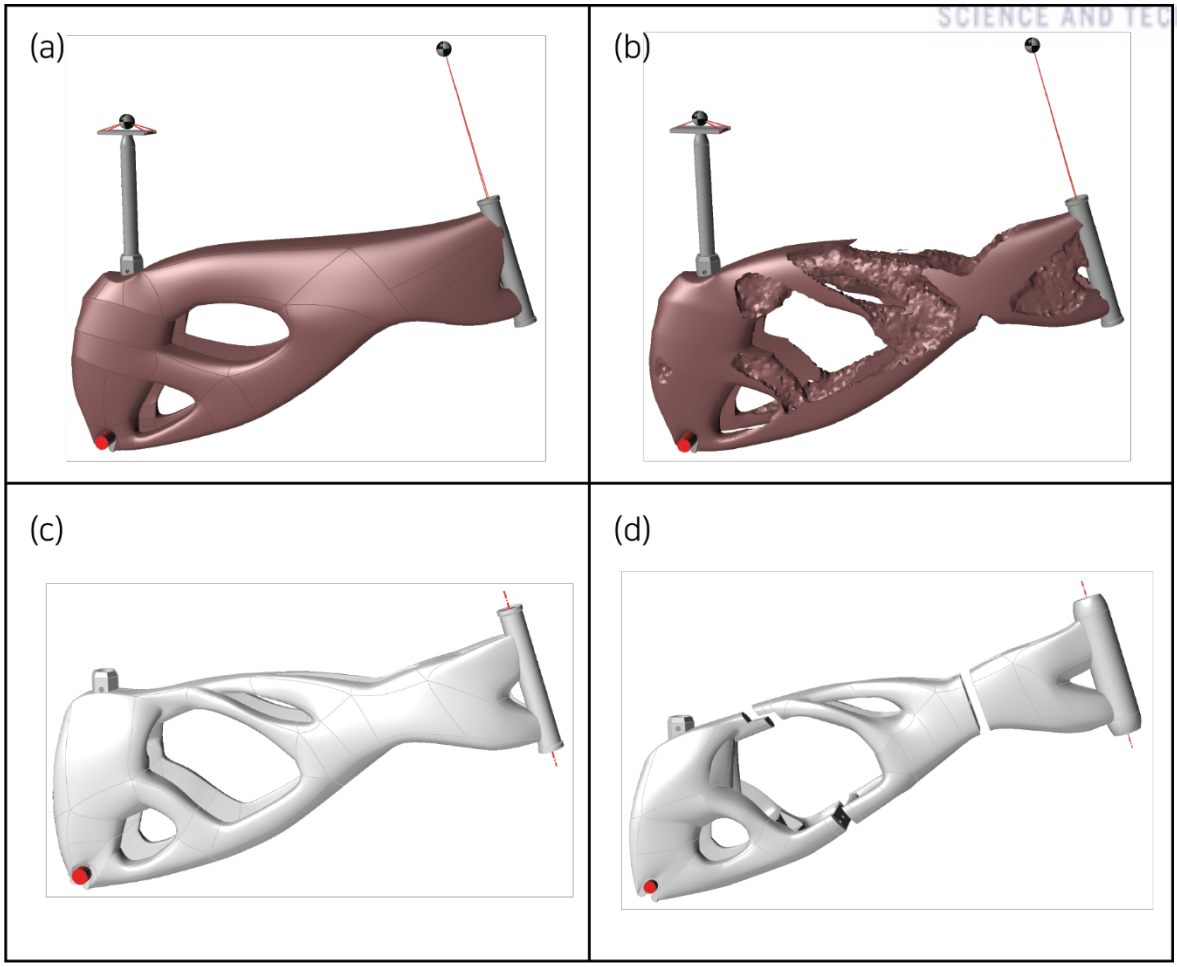

Figure 2.6 Topology Optimization Results (a) After First Optimization (b) After Second Optimization (c) After Design Post-processing (d) Final Optimization Result

Finally, in order to fully utilize the strength of additive manufacturing which is capable of fabricating complex structure, lattice structure was applied to the front and mid part of the frame to reduce weight while maintaining its stiffness. (Figure 2.7)

Figure 2.7 Applied Lattice Structures

- **Printing Procedure**

The complete assembly of SLS 3D printed electric bicycle is showed in Figure 2.8. The specification of the SLS machine used for the fabrication is described in

Table 2.1. For the SLS machine that is used for fabrication of the frame parts, the maximum printable part size is determined by the size of the powder bed. With the size of the machine, the frame was not able to be fabricated at once; the frame was divided into three parts (rear, mid and front) and fabricated separately with two batches. Orientations of batches are represented in Figure 2.9.a and b.

In Table 2.2, the configuration of the SLS machine is listed. Volume, weight and manufacturing time of frame parts are listed in Table 2.3.

Figure 2.8 Complete Assembly of 3D Printed Electric Bicycle

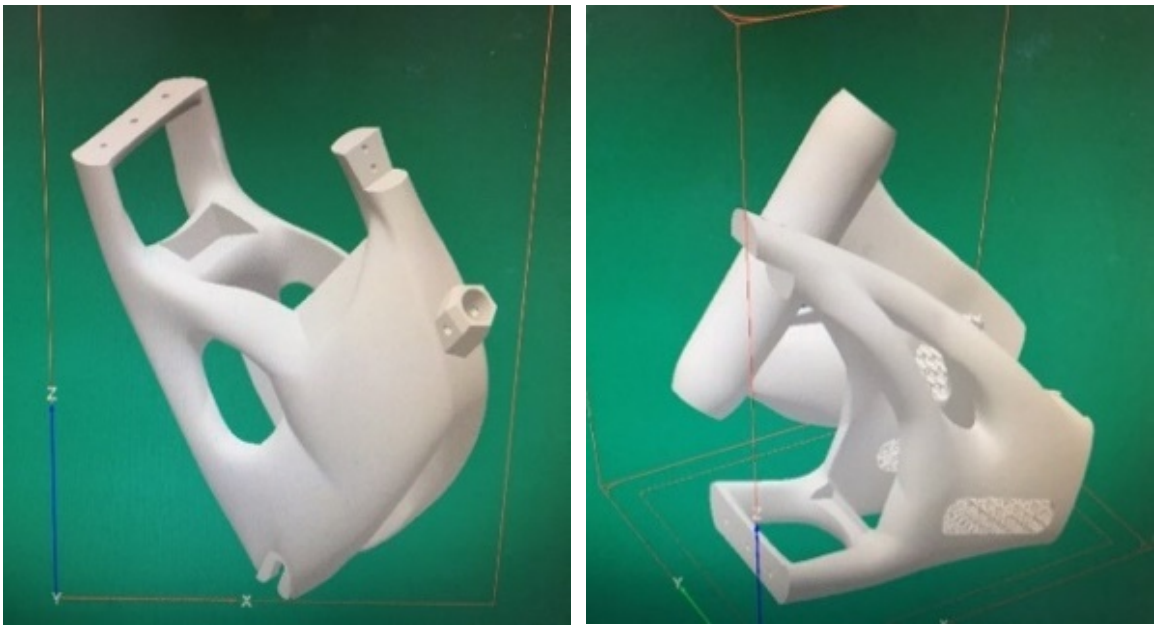

Figure 2.9 Part Batch Demonstration (a) Rear Part Batch (b) Mid & Front Part Batch

Table 2.1 3D Printer Specification

Platform	sPro60 SD
Manufacturer	3D Systems
Technology	Selective Laser Sintering
Min. Layer Thickness	0.08
Max. Build Size	$381 \times 330 \times 437$mm

Table 2.2 3D Printer Setting

	Rear Part	Front & Mid Part
Layer Thickness	0.1mm	0.12mm
Outline Laser Power	5W	6W
Fill Laser Power	18W	18W
Material Used	DuraForm PA	
Feed Temperature	135℃	
Bed Temperature	172.5℃	

Table 2.3 Print Result Information

	Rear Part	Mid Part	Front Part
Volume	3463.3cm^2	1704.7cm^2	1783.9cm^2
Weight	3.1kg	1.38kg	1.30kg
Mfg. Time	35 hours	31 hours	

- **Finite Element Analysis**

Similar to TO process, structural analysis was conducted using solidThinking Inspire® 2016. Figure 2.10 shows the graphical representation of the displacement of the frame when the same load case used for TO is applied to the frame. Darker color represents the higher displacement of the frame part. The maximum displacement of the frame is 7.588×10^{-5}m.

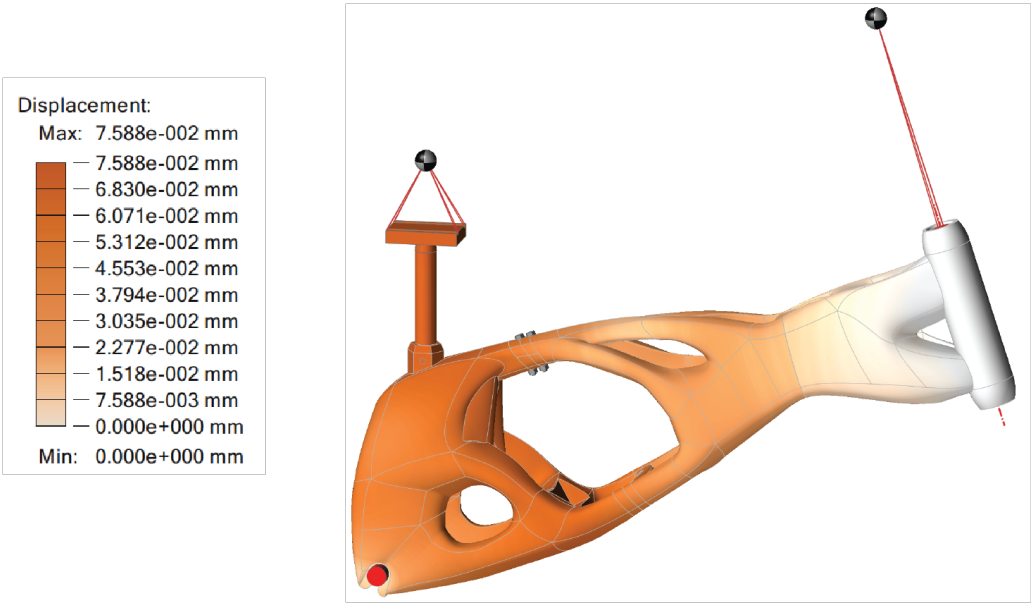

Figure 2.10 Graphical Representation of the Displacement of the Frame

2.4.4 Discussion

In this case study, the possibility of applying AM to the production of the final part was validated by actual design and manufacturing process of a new electric bicycle. DFAM concept was implemented to the design process of the bicycle frame, and the entire manufacturing process was conducted. By applying TO to the design process and FEA for the assessment of the prototype design, the design and modification cycle was completed in a short period of time. The entire process from the part design to the production was conducted within a week, and frame fabrication using SLS machine was carried out less than 70 hours.

The performance of the produced bicycle was compared to electric bicycles on the market that is generally around 20kg; it was able to reduce the weight of the electric bicycle about 17% resulting weight of the 16.5kg total. As the battery pack and the motor compartment comprise a majority of the total weight, it is expected that the weight of the frame part was reduced further. Also, although we conducted the structural analysis with the weight of the passenger as 100kg, which is harsher condition compared to the average weight of the adult, the safety factor was greater than 3.0 over the entire frame. Further improvement on the weight and stiffness of the frame structure is expected

if the TO is utilized more aggressively.

It is hard to conclude the marketability of the electric bicycle produced with the SLS process is feasible. Even though the structural performance can be improved further, the cost of SLS process is very high in the present, and the build volume of present SLS system is not large enough to produce a part such as a bicycle frame in a single batch. However, the build volume of the powder bed fusion system is increasing year by year (largest one is A.T.L.A.S from GE additive with the size of build envelope, $1{,}100 \times 1{,}100 \times 300\text{mm}$) and other kinds of material or AM process could be more suitable to produce the final part.

The role of DFAM turns out to be significant for the feasibility of the AM produced parts as the price for the SLS process is very expensive currently and the and thus design of effective and efficient structure is essential.

In the next chapter, an algorithm to generate lattice structure for the AM process is presented. The algorithm can help engineers to design lattice structures customized to a specific load case efficiently.

3. Methodology: Generation of Lattice Structure Using Topology Optimization of Unit Cells

As discussed in Chapter 2, topology optimization (TO) has great importance in DFAM. Since additive manufacturing does not guarantee superiority in cost and time for production of a large number of parts, part design should be carefully tailored for AM to maximize its strengths and advantages compared to conventional manufacturing methods.

3.1 Drawbacks of Topology Optimization Method

Topology optimization is an effective proven technology that has been developed for many years. Also, it is an essential technology for DFAM as it strengthens the advantages of AM. However, there are several limitations making it difficult to be implemented for general applications of AM.

First, TO requires the support of specialized CAE software and experts. Only specialized CAE programs support TO solution. Even if it is supported, for a proper TO integration to the AM process, an understanding of optimization process, finite element analysis or at least concepts of statics are required. Second, the TO problem requires a substantial amount of computation which takes a long time to be solved in a general computing system. Third, it requires long post-processing process. As the structure derived from TO is first expressed in density values varying from 0 to 1, penalization is used to obtain the outline of the structure, resulting structure being too rough to be implemented directly. Smoothing process for the TO-derived structure is essential where it takes a long time as an engineer to work with manually.

In this chapter, I suggest an algorithm to generate a lattice structure by stacking pre-optimized building blocks for various stress conditions. The algorithm can help to generate TO-derived lattice structure customized to load cases using less computational resource than general TO process.

3.2 Lattice Structure Generation Algorithm

3.2.1 Outline of the Entire Process

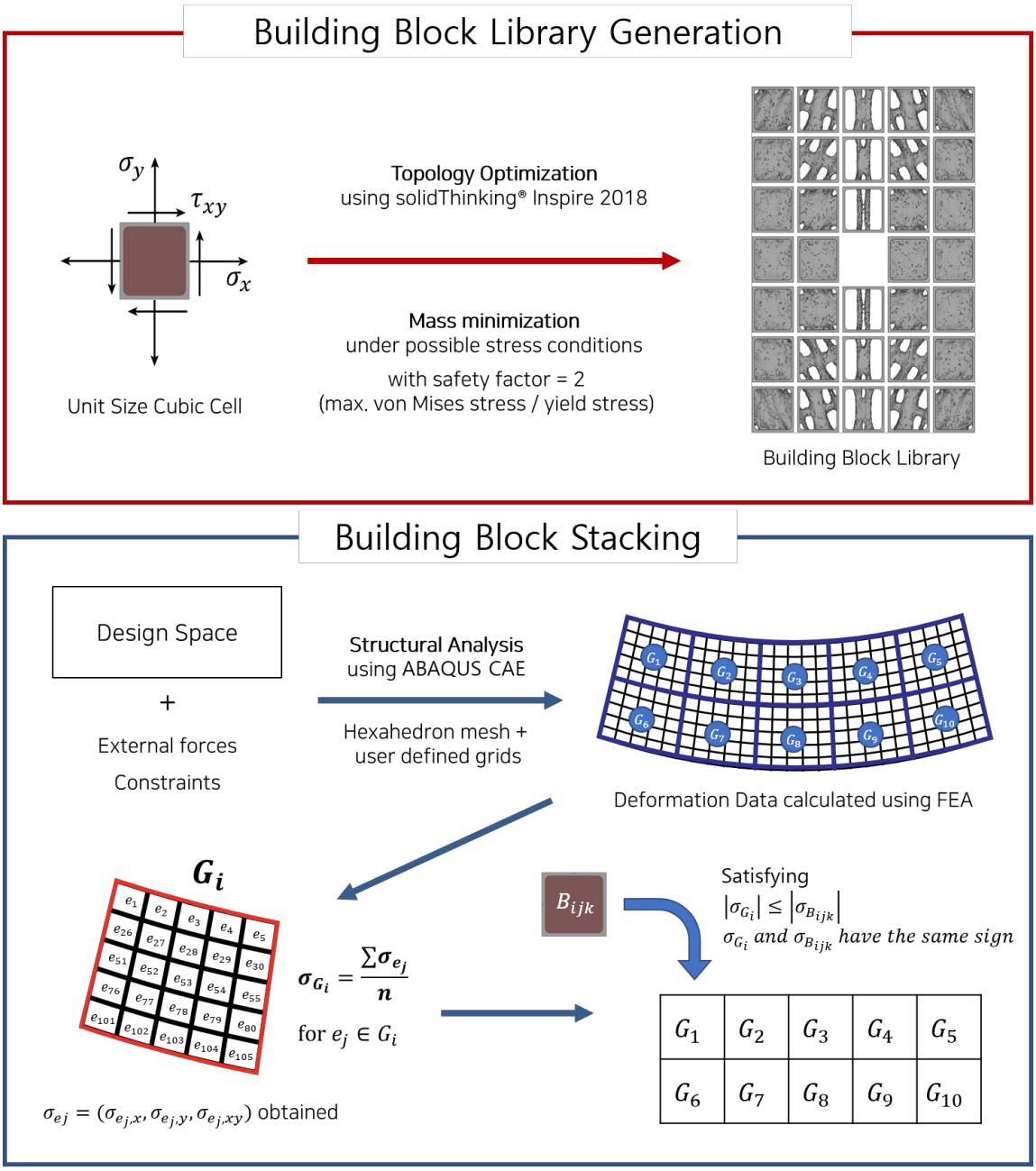

Figure 3.1 The Outline of the Lattice Structure Generation Method

The method is divided into two phases: Building Block library generation phase and stacking phase as illustrated in Figure 3.1. The method stacks the building blocks generated from building blocks generation phase to generate appropriate lattice structure for the design requirements.

In the building blocks generation phase, a unit cubic cell with fillets was prepared (Figure 3.2.a)

for TO under various stress conditions (Figure 3.2.b). In order to simulate the stress conditions that will be applied to the cell when it is stacked, normal and shear stresses were applied to the surfaces (right, left, top and bottom) of the cell as illustrated in Figure 3.2.b. Unit cells were topologically optimized according to the stress conditions applied using TO program, Optistruct, which is embedded in solidThinking Inspire software. As a result, 245 building blocks were generated using mass minimization method with a safety factor of 2. Each building block was optimized for specific stress condition and considered to be a proper cell structure for the stress condition.

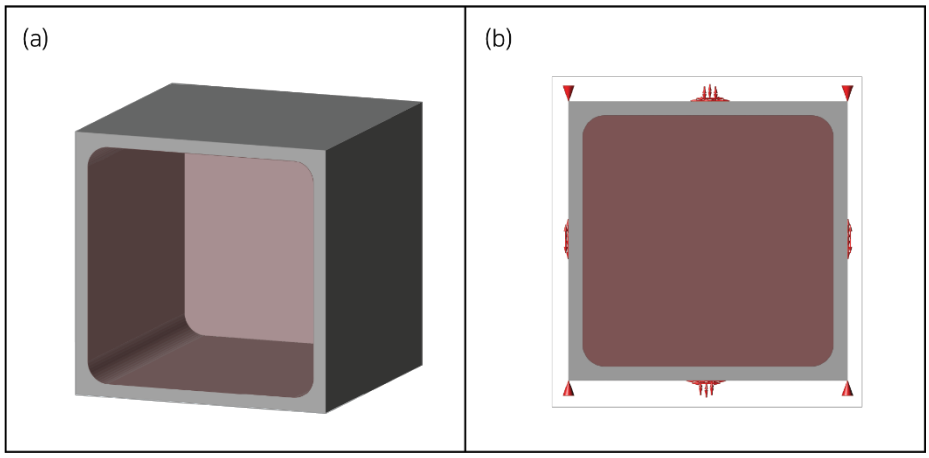

Figure 3.2 (a) Unit Cell Structure (b) Unit Cell Structure with Loads

In the building blocks stacking phase, a finite element analysis was conducted to the design space of the given problem using ABAQUS. The result from this initial analysis was used as a blueprint for the stacking process. The result data was extracted from .odb (output database) files using python scripts and prepared for the stacking process. According to the structural analysis data, MATLAB code was used to allocate a proper building block to each grid in the design space to generate a lattice structure.

After stacking building blocks, the resulting structure is post-processed and voxelized to generate an input file that can be read in ABAQUS to assess the performance of the lattice structures.

3.2.2 Building Block Generation Phase

For this suggested method, the building blocks, unit cell structures optimized to various stress conditions, had to be prepared. The basic geometry of building blocks was determined based on its requirements. First, the connectivity between building blocks should be guaranteed to make the lattice structure. Second, the inner space of the block needs to be customizable according to various stress conditions. It means inner space should have enough design space for TO. Third, the inner corners of the building block must be rounded. As unit cells are individually optimized and stacked to form a lattice structure, stress concentration can occur in the corner parts attached to other cells.

In order to alleviate the concentration and resulting problem caused by the area, inner corners of the building block were rounded.

A base cubic cell that has 4 surfaces (right, left, top and bottom side) and fillets was set for TO process) as shown in Figure 3.2. The inside of the cell was designated as a design space (transparent reddish-brown area). After several preliminary structural analysis on the initial design space, stress conditions applied to the cell structure for TO were determined as listed in Table 3.1. These stress conditions were determined so that they cover the stress responses of the actual structures. Since plane stress condition was assumed, only $\sigma_x, \sigma_y, \tau_{xy}$ components of stress tensor were considered. Total of 245 combinations of the three stresses were used as loading conditions which were written in .csv files using python scripts and imported to solidThinking Inspire software.

Table 3.1 Stress Conditions Applied to the Base Cell Structure

$\boldsymbol{\sigma_x}$	8	4	2	0	-2	-4	-8
$\boldsymbol{\sigma_y}$	4	2	1	0	-1	-2	-4
$\boldsymbol{\tau_{xy}}$		3	1.5	0	-1.5	-3	

In Figure 3.3, a schematic of the building block library generation phase is depicted. In the figure, TO process was expressed as a function with loading condition ($\sigma_x, \sigma_y, \tau_{xy}$). Each stress component was expressed with a_i, b_j, c_k as they can be varied. a_i was set from -8 to 8 MPa, b_j from -4 to 4 MPa, and c_k from -3 to 3 MPa. The optimized structures were expressed as B_{ijk}. Indices i, j, and k followed the same indices with stress components. The stress vector used to obtain the structure B_{ijk} was expressed as $\sigma_{B_{ijk}}$. Thus, the resulting structure generated with TO with stress a_i, b_j, and c_k could be expressed mathematically,

$$B_{ijk} = f\left(\sigma_{B_{ijk}}\right) = f(a_i, b_j, c_k) \qquad \textbf{Equation 3.1}$$

where $i = \{1,2,\cdots,n\}$, $j = \{1,2,\cdots,m\}$, $k = \{1,2,\cdots,l\}$. n,m, and l are numbers of stress variations.

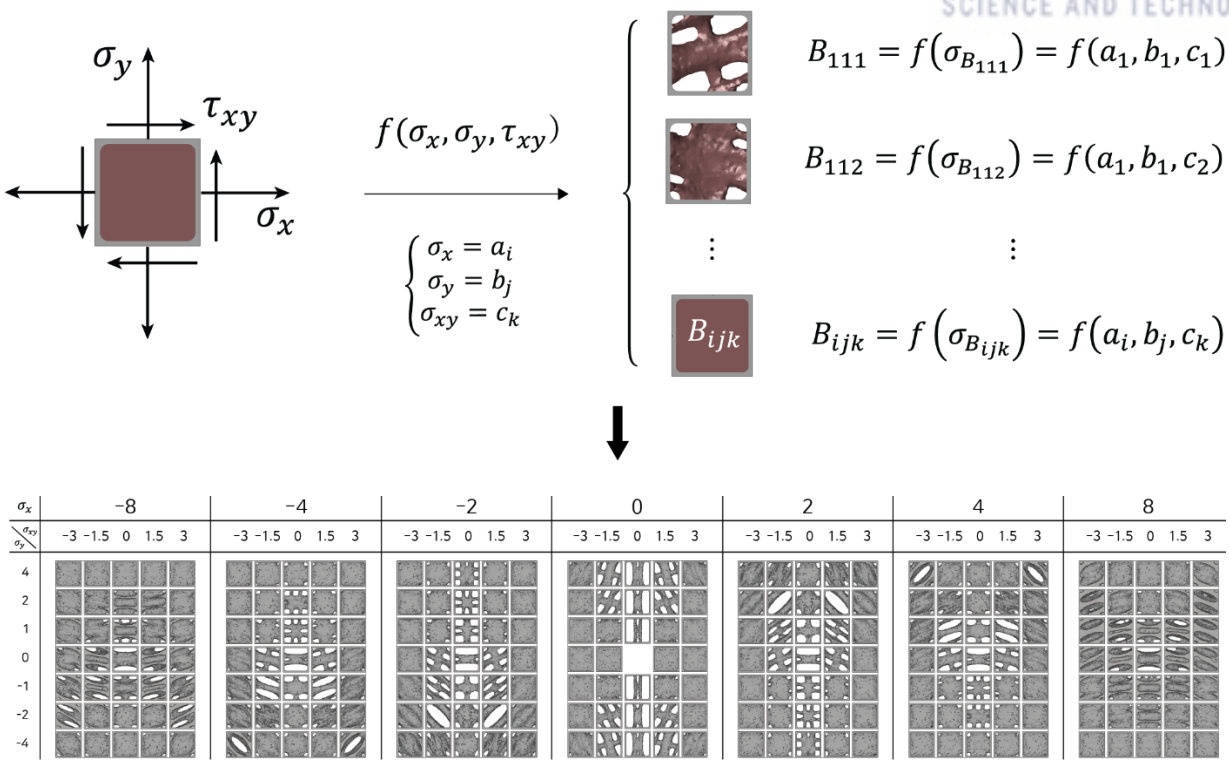

Figure 3.3 Schematic of Building Block Library Generation

Topology optimizations on the base unit cell with 245 load cases were conducted and listed in Appendix A.

3.2.3 Building Block Stacking Phase

Building block stacking phase starts with a particular design problem that has loads and constraints as illustrated in Figure 3.4. In this study, I focused on the design space that can be grided into cubic cells denoted by G_1 to G_{10} in Figure 3.4. The objective of the building block stacking phase is to fill the grids with proper building blocks that can endure stress condition induced by the loads and constraints of the problem.

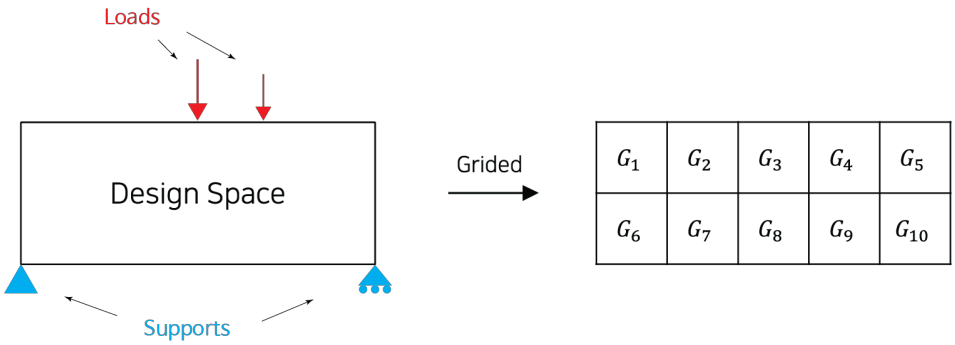

Figure 3.4 Schematic of Grid Generation

In order to obtain the stress distribution field that the design space will experience, FE analysis is executed on the problem. Through the FE analysis, a structure is meshed with 3-dimensional polygons such as tetrahedra or hexahedra (illustrated in Figure 3.5).

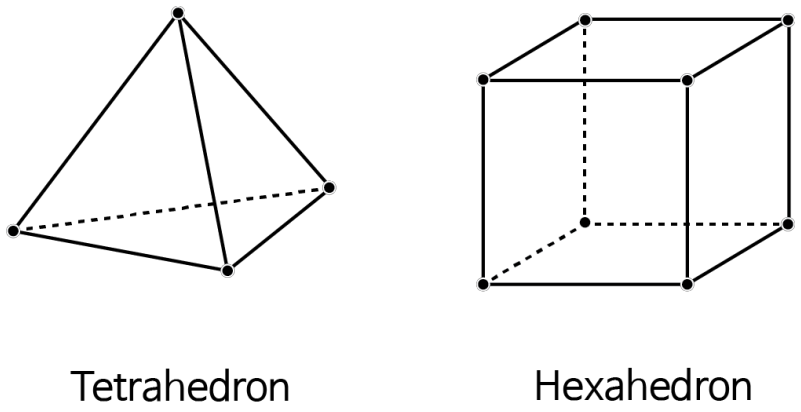

Figure 3.5 Types of 3D Solid Elements used in the FE Analysis

The basic governing equation of FEA on the structural analysis can be expressed as follows [25].

$$[\mathbf{K_S}]\{\mathbf{Q_S}\} = \{\mathbf{F_N} + \mathbf{F_T} + \mathbf{F_B}\} \qquad \textbf{Equation 3.2}$$

where $[\mathbf{K_S}]$ is the structural stiffness matrix, $\{\mathbf{Q_S}\}$ the displacement vector, $\mathbf{F_N}$ the nodal force vectors, $\mathbf{F_T}$ the traction force vectors, and $\mathbf{F_B}$ the body force vectors. By solving Equation 3.7, the displacement vectors of nodes are calculated. Also, the stress in an element can be obtained as follows.

$$\{\sigma\} = [\mathbf{C}]\{\epsilon\} = [\mathbf{C}][\mathbf{B}]\{\mathbf{q}^{(e)}\} \qquad \textbf{Equation 3.3}$$

where $[\mathbf{C}]$ is the elasticity matrix, $[\mathbf{B}]$ the constant related to the geometry of the element, and $\{\mathbf{q}^{(e)}\}$ the nodal displacement vectors. As stress is calculated element-wise, the stress state in an element is assumed to be homogeneous in FEA. Thus, the boundary where adjacent elements are connected has a stress difference between each element. The ambiguity of stress value can be alleviated by reducing the element size. When the size of the element decreases infinitesimal, the convergence of the stress value to the analytical solution is predicted. In reality, the use of infinitesimal elements results in infinite number of elements and infinite amount of time for the calculation. Thus, FEA users should compromise between the accurate solution and the computation time.

Due to the nature of FEA calculation, in order to get accurate stress values inside of the grids, elements smaller than grid size should be implemented. An example of deformed design space with elements and grids is given in Figure 3.6. As you can see in the figure, each grid is comprised of multiple elements. Element numbering is done regardless of elements, that means a grid can be

comprised of elements with discontinuous indices (element numbering was assumed to be from upper-left to lower-right in this figure).

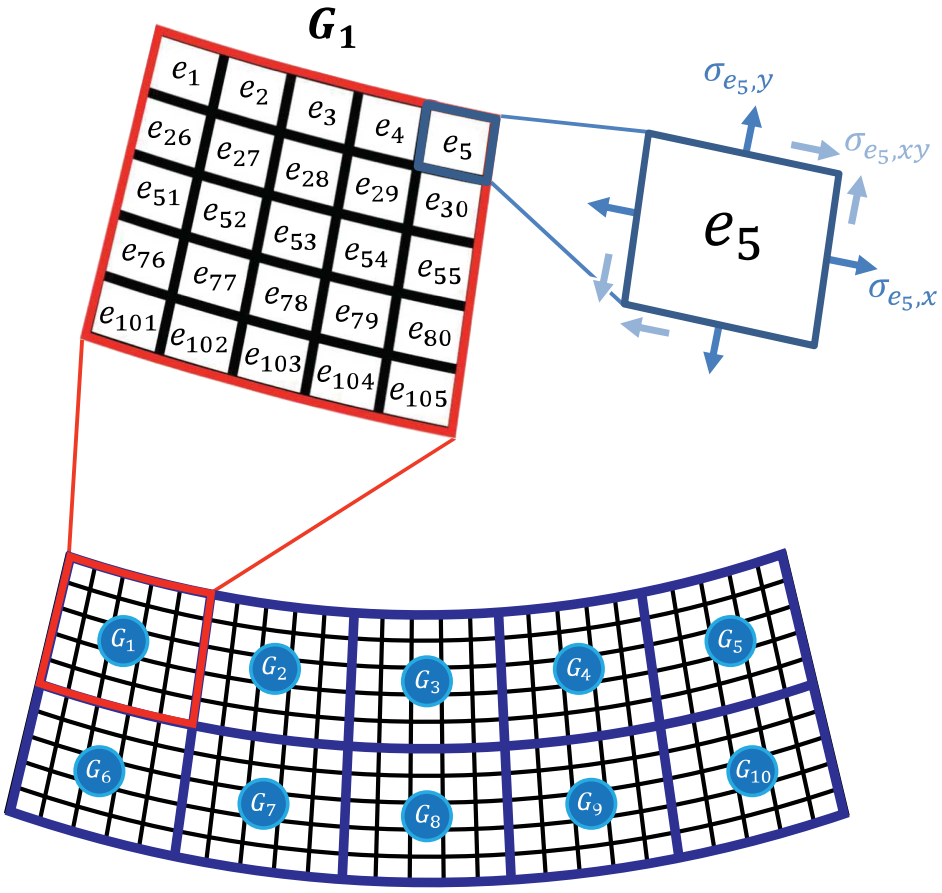

Figure 3.6 The Schematic of Deformed Design Space

The stress state of an element experience was expressed as,

$$\sigma_{e_p} = (\sigma_{e_{p,x}}, \sigma_{e_{p,y}}, \sigma_{e_{p,xy}}) \qquad \textbf{Equation 3.4}$$

where $p = \{1,2,\cdots,n\}$ with n being the total number of elements in the structure.

In order to calculate the representative stress of each grid, average stress value in the grid was calculated as follows.

$$\sigma_{G_s} = \frac{\sum \sigma_{e_t}}{m} \qquad \forall\, e_t \in G_s \qquad \textbf{Equation 3.5}$$

where m is the total number of elements in a grid.

Using the representative stress of each grid σ_{G_s}, a building block B_{ijk} that satisfies following the condition was determined for each grid.

$$\left|\boldsymbol{\sigma}_{\boldsymbol{G_{s,C}}}\right| \leq \left|\boldsymbol{\sigma}_{\boldsymbol{B_{ijk,C}}}\right|, \quad \boldsymbol{\sigma}_{\boldsymbol{G_{s,C}}} \cdot \boldsymbol{\sigma}_{\boldsymbol{B_{ijk,C}}} > \mathbf{0} \qquad \textbf{Equation 3.6}$$

where $\boldsymbol{C}$ denotes the component of the stress that is x,y, and xy in this case.

The first condition of Equation 3.7, $\left|\boldsymbol{\sigma}_{\boldsymbol{G_{s,C}}}\right| \leq \left|\boldsymbol{\sigma}_{\boldsymbol{B_{ijk,C}}}\right|$ means that the component-wise stress condition of TO that the building block was optimized should be larger than the representative stress of the grid regardless of the sign of the stress. The second condition of Equation 3.7, $\boldsymbol{\sigma}_{\boldsymbol{G_{s,C}}} \cdot \boldsymbol{\sigma}_{\boldsymbol{B_{ijk,C}}} > \mathbf{0}$ means that the sign of the stresses should be the same because building block should bear the stress condition the grid experience.

Using the above conditions, building blocks that can endure the stress condition of the design problem are chosen to fill the grids. The selected building blocks are stacked and form a lattice structure.

3.2.4 Summary of the Suggested Lattice Structure Generation Method

The flowchart of the suggested lattice structure generation method is illustrated in Figure 3.7. As can be seen in the figure, the actual generation process begins with the structural analysis of the design space. The structural analysis was conducted in the ABAQUS software, but any FEA software can be utilized as long as the model data and result data can be provided. From the model data, element number and element position data are obtained, and from the result data, element number and element stress data are extracted (the python script used for the access of ABAQUS output database file is presented in Appendix C).

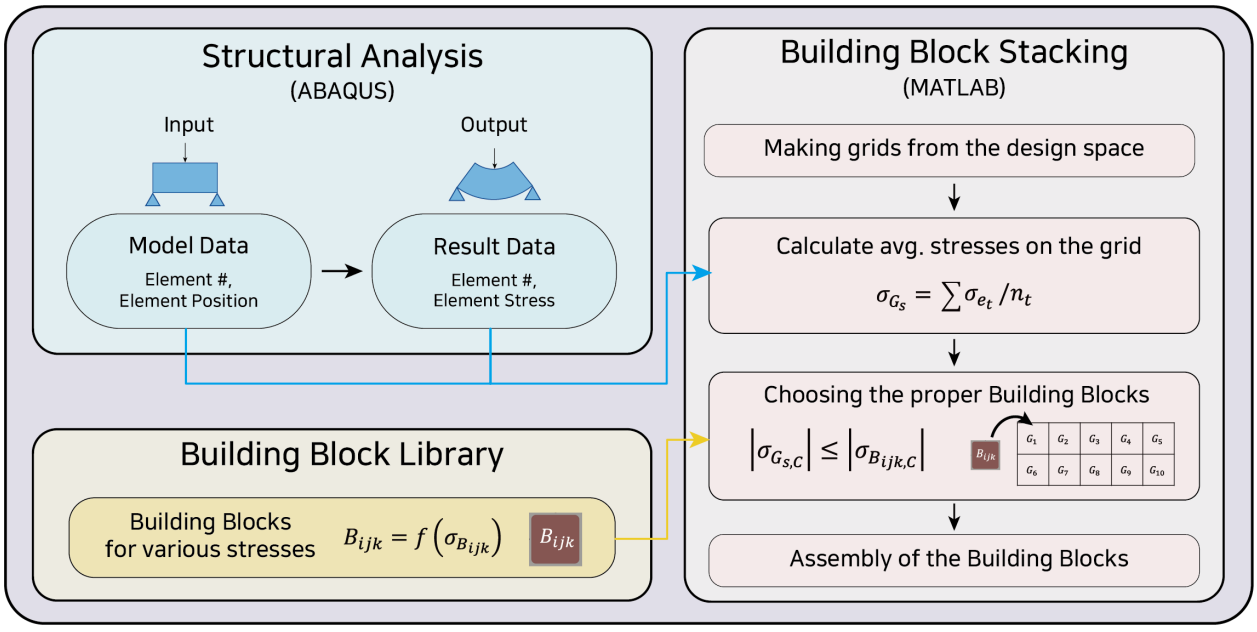

Figure 3.7 The Flowchart of the Suggested Lattice Structure Generation Method

The actual calculation of average stresses on the grids, selection of proper building blocks, and assembly of the final structure are performed in MATLAB. The MATLAB code, found in

Appendix D makes the grids from the design space and calculates the average stresses on the grid by using the model data and result data obtained from the ABAQUS analysis.

After calculating average stress vectors in the grids, the stress vectors are compared with the stress conditions implemented to the generation of building blocks. The building blocks optimized with the greater stress condition (component-by-component, with the same sign) are chosen for the generation of the lattice structure.

Assembly of the building blocks (that are .stl files) also has been implemented in MATLAB code. The resulting lattice structure file was generated in .stl file format which is one of the most frequently used formats in AM. Thus, the suggested method can be easily implemented to the AM method.

3.3 The Result of the Structure Generation

3.3.1 Case Study – Bridge

The case study was conducted to compare the suggesting algorithm with existing TO process. In this example, a simple bridge problem was considered as represented in Figure 3.8. A bridge is designed as a rectangular solid with the size of $220\text{mm} \times 40\text{mm} \times 20\text{mm}$ (Width × Height × Depth). Then, it is supported by two plates at both ends, and a load is exerted at the middle by the same plate used as supports.

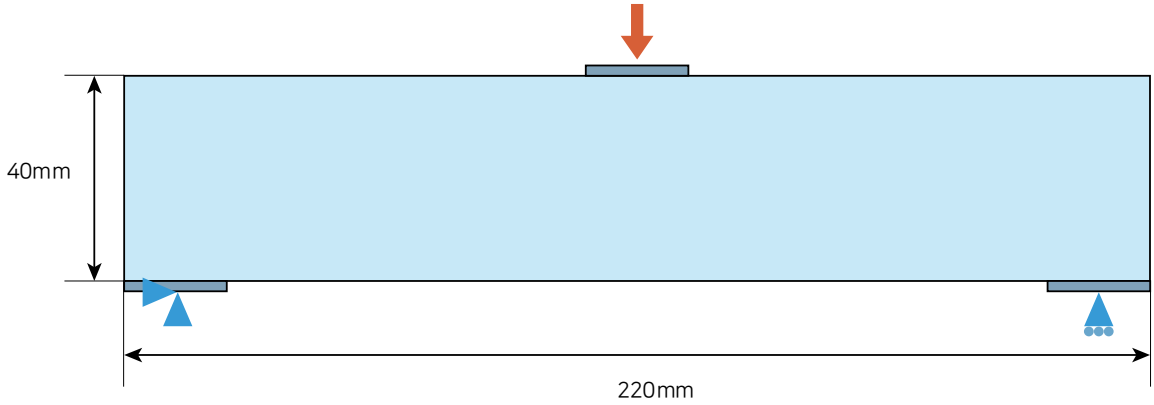

Figure 3.8 The Schematic of Design Space and Load and Support Condition

Plates are assumed to be rigid bodies. The left end of the bridge is constrained for any translational displacement, and the right end of the bridge is constrained for vertical and depth-direction translation so that the bridge can be deform in horizontal direction when the load is applied. The material of the bridge is engineering plastic (Acrylonitrile Butadiene Styrene) with 2GPa of Young's modulus, 45MPa of yield stress and 1.06 kg/m^3 of density values.

The size of the plate is 20mm × 20mm (width × depth) with 2mm thickness. In finite element analysis, the supports and the load are applied to the contacting surface between the plates and the bridge.

In order to generate a lattice structure with presented method, the design space needs to be gridded with the size of the building block. In this example, the size of the building block is 20mm × 20mm × 20mm while the size of the design space is 220mm × 40mm × 20mm. Thus, the entire structure is composed of 22 building blocks total (Figure 3.9). Filling in each grid with proper building block is the key to generating a sturdy structure according to applied loads.

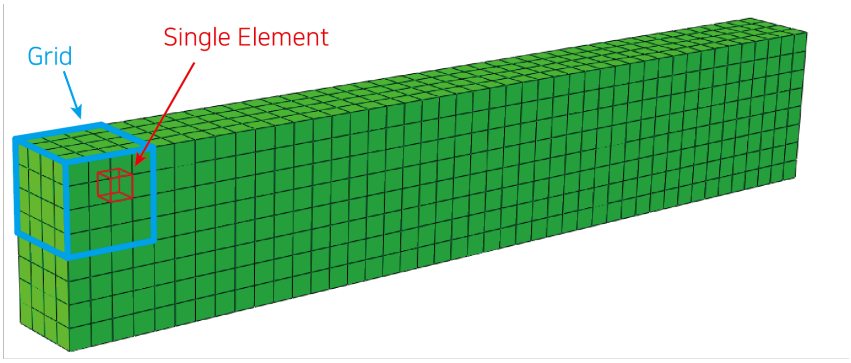

Figure 3.9 Representation of Grids and Elements in the Structure

As described in the previous section, the structural analysis data was used to obtain the stress data in the grids as illustrated in Figure 3.10. Structural analysis was performed in ABAQUS, which is a well-known FEA software. Since the initial design space has a simple geometry, the analysis was performed in a short time. The ABAQUS analysis result was saved as .odb file. Then, it was possible to extract the stress vector from each element using ABAQUS command prompt, also supported by ABAQUS.

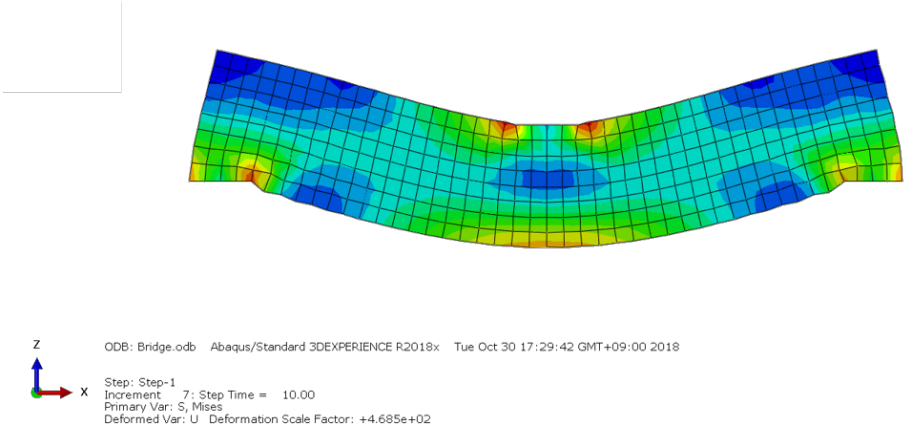

Figure 3.10 Deformed Structure Calculated in ABAQUS

Selection of the building blocks for the grids was done by comparing the average value of the stress vectors in the grid with the stress vector used for TO process of each building block. In order to guarantee that each building block endures the given stress condition, a TO process was done with mass minimization method with a safety factor of 2, meaning virtually the building block can endure stress twice bigger than the given stress condition. Also, the algorithm was written in a way that the stress endurance limit of each building block always exceeds the average value of stress tensors in the grid so that the building block doesn't fail at all time.

The lattice structure generated with the method is presented in Figure 3.11. The structure was voxelized using MATLAB code, and static analysis was conducted using ABAQUS software as illustrated in Figure 3.12. The maximum displacement and von Mises stress from the result are listed in Table 3.2.

Figure 3.11 Lattice Structure Generated with the Suggesting Algorithm

Figure 3.12 The Structural Analysis Result of the Lattice Structure Generated with the Suggesting Algorithm

In order to compare the result with a general TO process, the design space was optimized by a method of compliance minimization with 50% volume constraint option under the same supports and load condition using the TO software solidThinking® Inspire 2018 (Figure 3.13). After the

optimization, structural analysis was conducted as shown in Figure 3.14. The model is colored with emerald for the regions experiencing the compressive stress and orange for the regions experiencing the tensile stress.

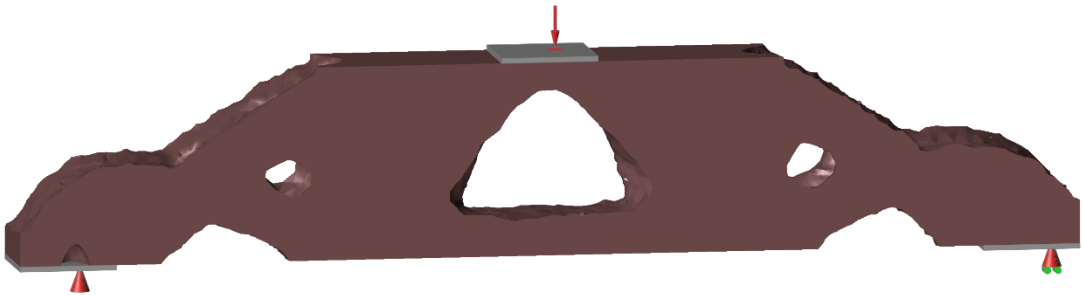

Figure 3.13 Topologically Optimized Structure using solidThinking® Inspire 2018

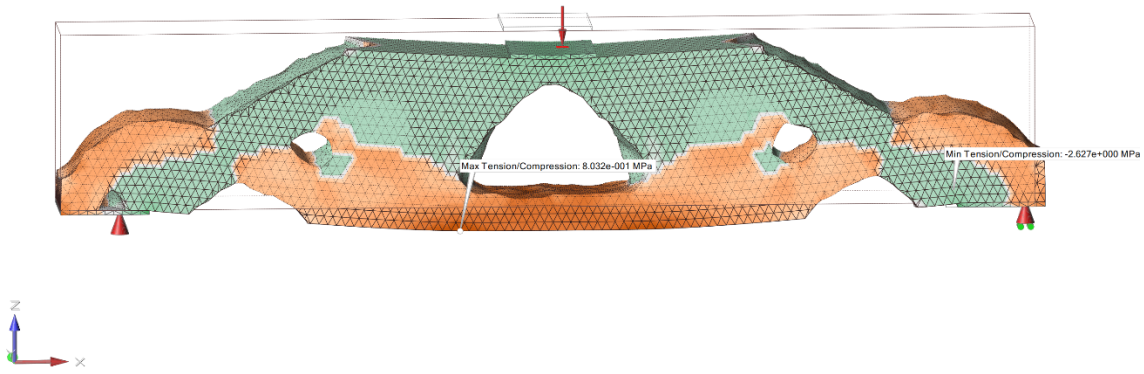

Figure 3.14 The Structural Analysis Result of the Topologically Optimized Structure

Comparison between original design space, general TO and suggested algorithm is done listing the results in Table 3.2. Elapsed time to generate the optimized structures were 4779 seconds for general TO process and 74 seconds for the suggested algorithm. As the suggested algorithm uses pre-optimized building blocks, so the stacking process only determines which building block is proper for each grid and merely allocate each block to the grid, the whole process does not require much computation. Estimated weight of the structure was calculated based on the voxels that comprise the structures. As a voxel is a cubic element, the volume of the entire structure was calculated by multiplying the volume of a voxel by the number of voxels in the structure. Resulting weights were estimated 93.56g for general TO structure and 94.51g for the structure made with suggesting algorithm.

Table 3.2 The Specification of Computer System and Results of Structural Analysis

Structure Generation Method	Design Space	Topology Optimization	Suggested Method
Computer System	Intel® Core™ i7-8700k CPU @ 3.7GHz, 64GB RAM		
Estimated Weight	186.56g	93.56g (49.8% ↓)*	94.51g (49.3% ↓)*
Maximum Displacement	0.05147mm	0.0786mm (52.7% ↑)*	0.1126mm (118.8%↑)*
Maximum Stress	5.687 MPa	2.627 MPa (53.8% ↓)*	3.205 MPa (43.6% ↓)*
CPU Time	-	4779 seconds	74 seconds (98.5% ↓)**

* : compared with Design space

** : compared with General TO result

Compared with TO structure, suggesting algorithm generates a less optimal structure, but the maximum displacement was less than the TO model. It means the effective stiffness of the structure is higher than the TO model.

However, the difference in elapsed time spent by two different methods is dramatic. Suggested algorithm showed more than 98% reduction in elapsed time which imply that this method is highly effective in generating quasi-optimized lattice structure in a short period of time. Overall, the purpose of the algorithm was fulfilled as it was designed to be an easy tool to generate optimized lattice structure for general AM users.

3.3.2 Case Study – Bracket

Another case study was conducted with bigger model. In this example, a simple bracket is considered as shown in Figure 3.15. The bracket is designed as a rectangular box with the size of $500\text{mm} \times 400\text{mm} \times 100\text{mm}$ (Width × Height × Depth). On the left surface of the bracket, two supporting plates are attached, and a load is exerted on the plate placed at lower right corner of the bracket.

The upper end of the bracket is constrained for any translational displacement while the lower end of the bracket is constrained for horizontal and depth-direction translation so that the bracket can deform to the vertical direction when the load is applied. The material of the bracket is assumed to be the ABS plastic.

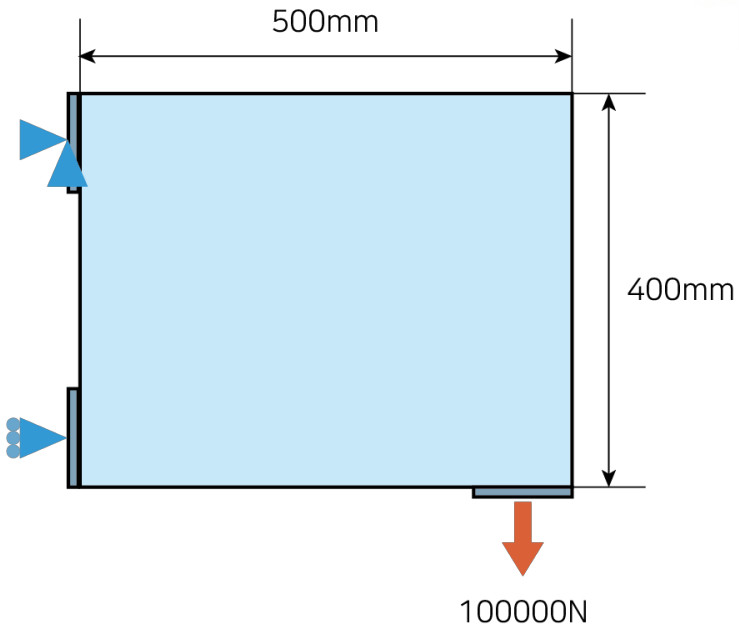

Figure 3.15 The Schematic of Design Space and Load and Support Condition

The size of the building block is set 100mm each side, and the size of the design space is 500mm × 400mm × 100mm. Thus, the entire structure is composed of 20 building blocks total.

Same with the previous case, the structural analysis data of the design space (Figure 3.16) was used to calculate the average stress in each grid and select the proper building block.

Figure 3.17 shows the lattice structure generated with the method. The structure was voxelized using MATLAB code, and static analysis was conducted using ABAQUS software. The analysis result is presented in Figure 3.18.

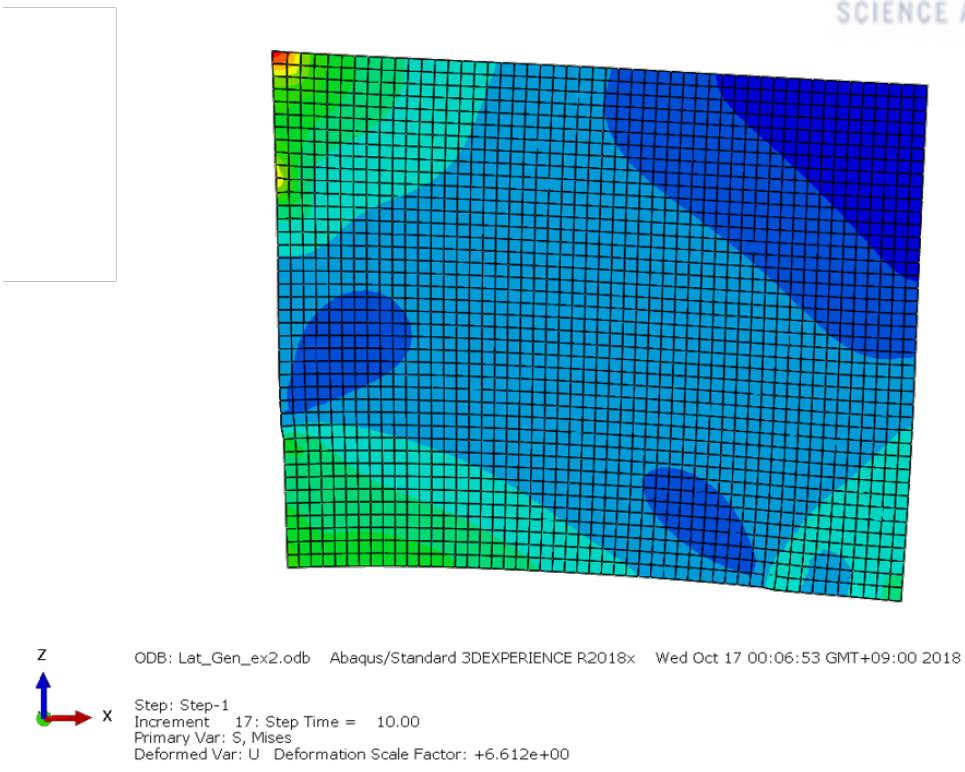

Figure 3.16 Deformed Structure Analyzed in ABAQUS

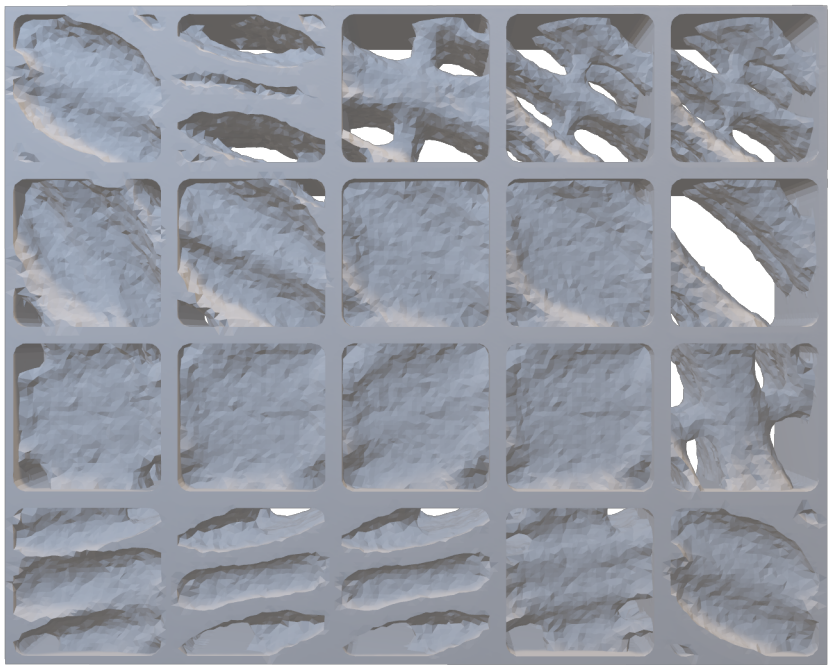

Figure 3.17 Lattice Structure Generated with the Suggesting Algorithm

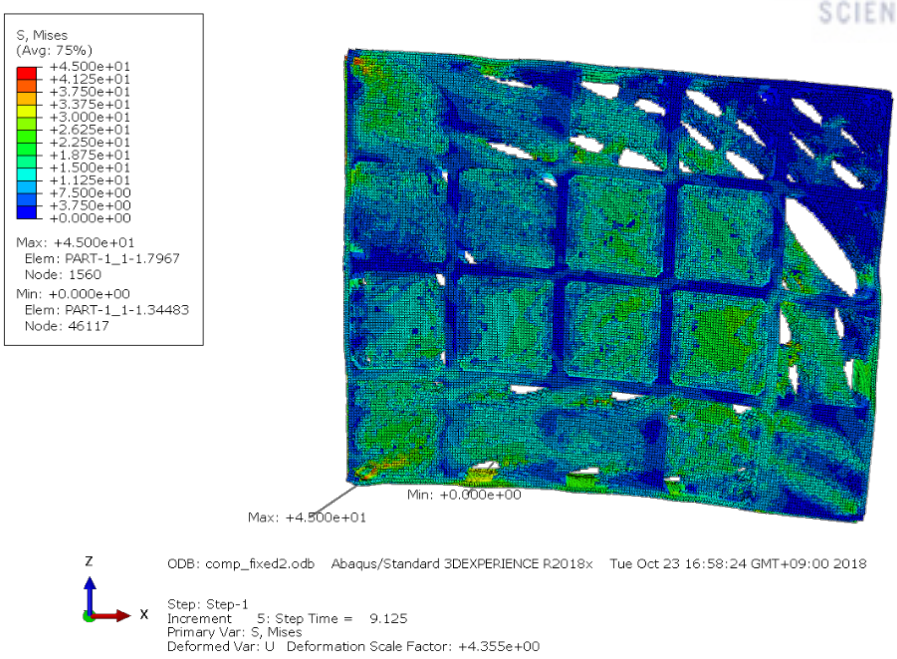

Figure 3.18 The Structural Analysis Result of the Lattice Structure Generated with the Presented Method

In order to compare the result with a general TO process, the design space was optimized with the same conditions used previously (Figure 3.19). After the optimization, structural analysis was conducted as shown in Figure 3.20. The model is colored with emerald for the regions experiencing the compressive stress and orange for the regions experiencing the tensile stress.

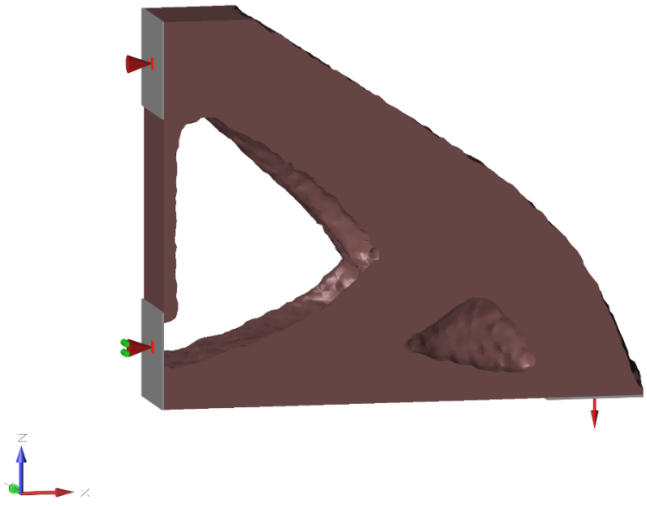

Figure 3.19 Topologically Optimized Structure using solidThinking® Inspire 2018

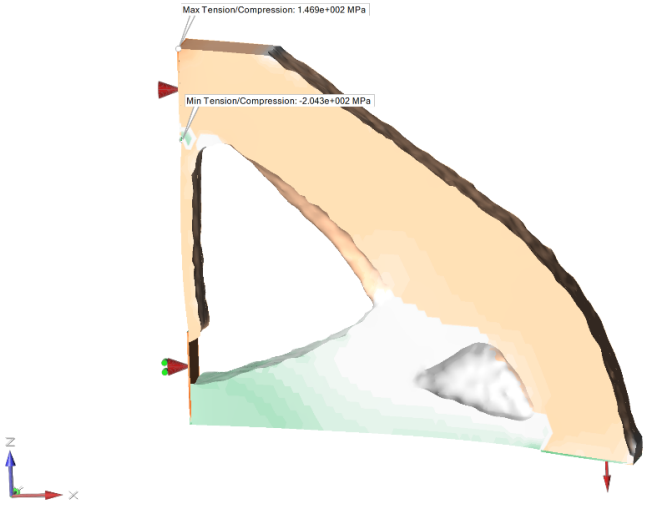

Figure 3.20 The Structural Analysis Result of the Topologically Optimized Structure

Comparison between original design space, general TO and suggested algorithm is made as presented in Table 3.3.

Table 3.3 The Specification of Computer System and Results of Structural Analysis

Structure generation method	Design Space	Topology Optimization	Suggested method
Computer system	Intel® Core™ i7-8700k CPU @ 3.7GHz, 64GB RAM		
Estimated Weight	21.2kg	10.572kg (50.1% ↓)*	12.19kg (42.5% ↓)*
Maximum Displacement	23.93mm	11.70mm (51.1% ↓)*	13.41mm (44.0% ↓)*
Maximum Stress	1651 MPa	204.3 MPa (87.6% ↓)*	77.8 MPa (95.3% ↓)*
CPU Time	-	2026 seconds	41 seconds (98.0% ↓)**

* : compared with Design space

** : compared with General TO result

Similarly with the result from bridge case, the result showed that the suggested method is less desirable in the aspect of effective stiffness compared to the structure generated with TO.

However, the elapsed time for the generation of the structure could be dramatically reduced again. Suggested algorithm showed an almost 98% reduction in elapsed time.

3.4 Discussion – A Way to Reduce the Amount of Building Blocks Required to be Generated

Topology optimization was performed under245 stress conditions to the unit cell structure and two kinds of symmetry in the structures were found. In this section, the reasons of the symmetries are explained with the Mohr's Circle. The symmetric property of the optimized structures can be utilized to reduce the number of the building blocks needed to prepare the library.

The optimized structures show symmetries by the sign of its shear stress and the combination of normal stresses. In Figure 3.3 (also in the Appendix for larger images), structures are grouped with the same x-directional normal stresses. As you can see, in each group, the structures are vertically symmetrical. Structures in the middle column are structures with no shear stress and columns on the right and left structure with a positive and negative value of shear stress respectively. Thus, they show vertically symmetrical structures according to their sign of shear stress.

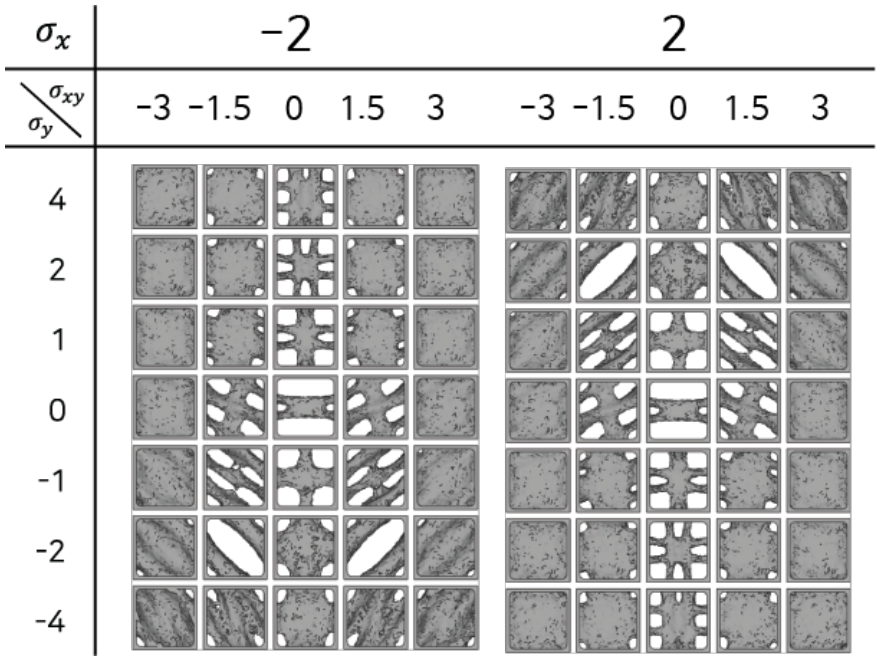

Figure 3.21 Building Blocks with X-directional Normal Components of the Stress = -2, 2

Also, another symmetry is found in the structures. In Figure 3.21, there are two groups of structures with x-directional normal stresses that are +2 and -2. As the middle row of the groups has no y-directional stress and rows on the upper side and lower side are structures with a positive

and negative value of y-directional normal stresses, you can find that structures with the same magnitude of x and y directional normal stresses with different sign show horizontally symmetrical structures.

The symmetries described can be explained with Mohr's circle for plane stress [26]. Mohr's circle is a graphical representation method of stress status in an element first introduced by German engineer Otto Mohr. Plane stress condition is represented as Figure 3.22. General stress status with tension represented in Figure 3.22.a can be redrawn with Mohr's circle representation shown in Figure 3.22.b. With normal compressive stresses, the circle locates on the left side to the vertical axis, and when compression and tension are applied at the same time, the vertical axis locates between the maximum abscissa of the circle and minimum abscissa of the circle. As we can see in the figure, the principal stress condition can be found readily using Mohr's circle. After finding the point where the stress condition locates (point X), we can find the angle θ by using the geometrical relationship of the triangle ACX.

$$\tan(2\theta_p) = \frac{\tau_{xy}}{\frac{1}{2}(\sigma_x - \sigma_y)} \qquad \textbf{Equation 3.7}$$

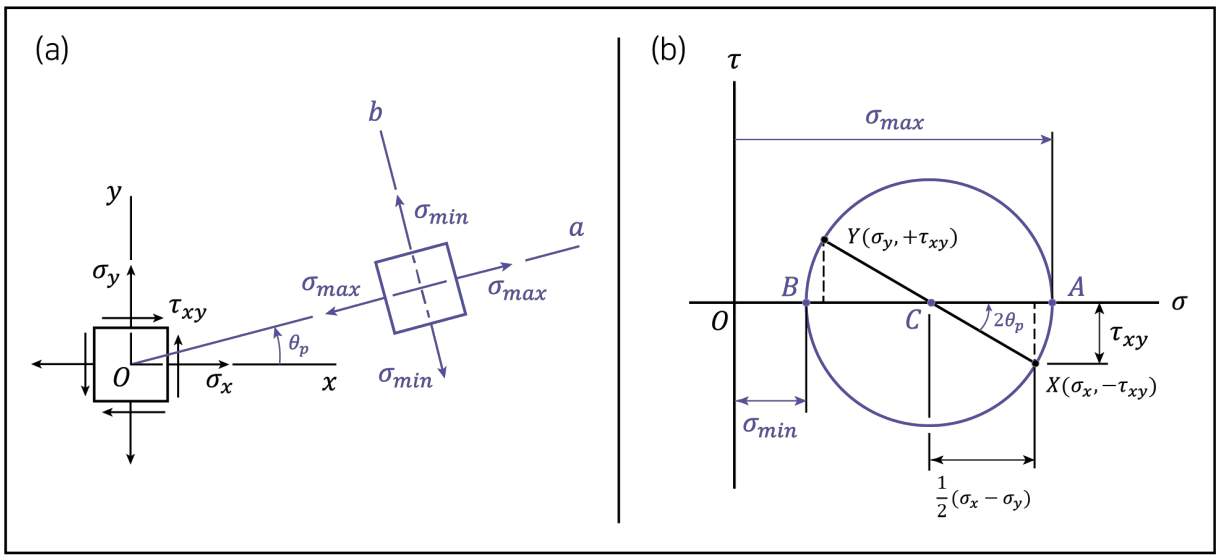

Figure 3.22 (a) General Stress Status of an Element with Principal Stresses σ_{max} and σ_{min} (b) Mohr's Circle Representation of the General Stress Status

According to the sign convention used in Beer et al.[26], positive shear stress is located below the horizontal axis, and negative shear stress is located above the horizontal axis.

When comparing stress conditions that have the same normal stresses and shear stresses with the

same magnitude and different sign, we can see that the two stress conditions can be represented as a Mohr's circle (Figure 3.23). It means that the two stress conditions have the same principal stresses when they are rotated the same angle θ by opposite directions. This explains why the structures, when applied opposite shear stress, shows vertically symmetry.

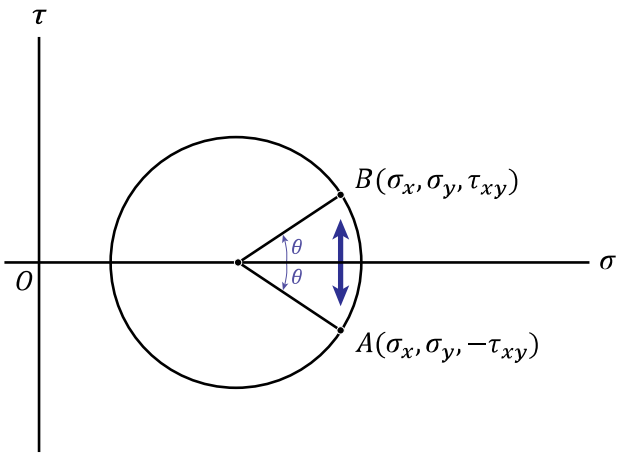

Figure 3.23 Two Stress States with Different Sign of Shear Stress Located in the Same Mohr's Circle

Stress conditions with opposite signs of normal stresses can be explained with Mohr's circle as well. In this case, two Mohr's circles that are equally spaced from the vertical axis are drawn according to the stress conditions as the right-hand side, and the left-hand side of the horizontal axis represent tensile and compressive stress respectively as illustrated in Figure 3.24. The two of Mohr's circles are vertically symmetrical and, when strain to the tensile and compressive loadings on the material is the same (linear elastic material), the stress conditions can be considered the same.

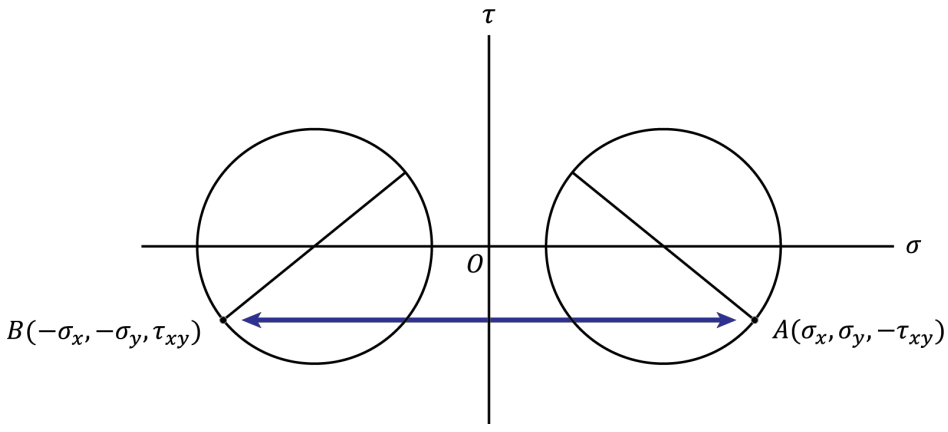

Figure 3.24 Two Mohr's Circles that are Equally Spaced from the Vertical Axis

Considering the finite element analysis and the TO process are done assuming the material is linear elastic material, the symmetry of structures with opposite signs of normal stresses is

reasonable.

Utilizing the symmetric characteristics of the structures, the amount of computation for the building blocks generation process can be reduced to the one-fourth compared to the original settings. Since structures with more similar stress condition to the stress distribution data can be chosen when structures with detailed stress conditions are prepared, the lattice generation algorithm can be improved by an extensive library of structures.

4. Conclusion and Future Works

4.1 Conclusion and Contribution

In this thesis, as a solution for universal applications of TO and DFAM methods in AM, a lattice structure generation method was developed and assessed by comparing its results with that of the existing TO method.

The presented method uses a library of building blocks that are pre-optimized with various stress situations and stacks the building blocks according to the analysis data of each design problem. As TO method which demands great amount of computational resources is performed in advance and users only deal with the stacking process, the design process can be greatly simplified reducing the time spent on the structure generation significantly. I also strongly suspect an improved effective stiffness by implementing larger building blocks library, meaning an overall improvement in performance.

Considering that the general public may not have great computational resources, specialized and expensive software, and knowledge of FEA or TO concepts, the presented method is a decent alternative for the existing design method.

4.2 Future Research

The lattice structure generation method presented in this thesis is developed with many assumptions, so this method can be further developed in many aspects.

1. The method was validated only with computer simulations. In order to obtain more accurate data on the stress response of the built structures, mechanical testing of actual manufactured structure will be needed.
2. The method is developed to be applied to the fabrication of final parts using AM. Case studies on the actual applications need to be made to validate the method.
3. As the method was developed for general AM users, each building block should be AM-applicable. The building block generation using TO with constraints related to the AM manufacturability (overhang restriction, minimum thickness criterion) needs to be studied.
4. As the building blocks were set to be cubic cells with 4 sides, the connectivity between building blocks could be guaranteed only for the rectangular design space. More adaptable building blocks need to be studied.

5. The method covers only 2D problem. Thus, plane stress is assumed. The method needs to be extended to the 3D condition to make it applicable to real cases.
6. The process of selecting proper building blocks in the method needs to be studied. In the method, the proper building blocks are determined by simple inequation comparing the stress condition of the TO that building block went through and the average stress on the grid for the design problem. The resulting structures show decent performance on the result but do not guarantee the building blocks chosen are the best combination of the blocks for the design problem. Study on how to search the best combination of the building blocks are needed for the further investigation.
7. As the method directly uses the stress distribution data from the structural analysis of the design space that changes with the structure, the optimization of the structure on the stress distribution is not accurate. That is the reason why TO requires iterations to get the optimized structure. Multi-step method on the structure generation can be applied to improve the method further.

References

1. *Standard Terminology for Additive Manufacturing – General Principles – Terminology*. 2015, ASTM.
2. Campbell, T., et al., *Could 3D Printing Change the World?: Technologies, Potential, and Implications of Additive Manufacturing*. 2011, Atlantic Council.
3. Petrovic, V., et al., *Additive layered manufacturing: sectors of industrial application shown through case studies.* International Journal of Production Research, 2010. **49**(4): p. 1061-1079.
4. Ko, H., S.K. Moon, and J. Hwang, *Design for additive manufacturing in customized products.* International Journal of Precision Engineering and Manufacturing, 2015. **16**(11): p. 2369-2375.
5. Nickels, L., *3D printing the world's first metal bicycle frame.* Metal Powder Report, 2014. **69**(2): p. 38-40.
6. *Wohlers Report*. 2018, Wohlers Associates. p. 173-174.
7. Conner, B.P., et al., *Making sense of 3-D printing: Creating a map of additive manufacturing products and services.* Additive Manufacturing, 2014. **1-4**: p. 64-76.
8. Yang, S. and Y.F. Zhao, *Additive manufacturing-enabled design theory and methodology: a critical review.* The International Journal of Advanced Manufacturing Technology, 2015. **80**(1-4): p. 327-342.
9. Rännar, L.E., A. Glad, and C.G. Gustafson, *Efficient cooling with tool inserts manufactured by electron beam melting.* Rapid Prototyping Journal, 2007. **13**(3): p. 128-135.
10. Liu, Z., et al., *Acoustic properties of a porous polycarbonate material produced by additive manufacturing.* Materials Letters, 2016. **181**: p. 296-299.
11. Wang, C., et al., *Concurrent topology optimization design of structures and non-uniform parameterized lattice microstructures.* Structural and Multidisciplinary Optimization, 2018. **58**(1): p. 35-50.
12. Andreassen, E., B.S. Lazarov, and O. Sigmund, *Design of manufacturable 3D extremal elastic microstructure.* Mechanics of Materials, 2014. **69**(1): p. 1-10.
13. Atzeni, E. and A. Salmi, *Economics of additive manufacturing for end-usable metal parts.* The International Journal of Advanced Manufacturing Technology, 2012. **62**(9-12): p. 1147-1155.
14. Ponche, R., et al., *A new global approach to design for additive manufacturing.* Virtual and Physical Prototyping, 2012. **7**(2): p. 93-105.
15. Moon, S.K., et al., *Application of 3D printing technology for designing light-weight unmanned aerial vehicle wing structures.* International Journal of Precision Engineering and Manufacturing-Green Technology, 2015. **1**(3): p. 223-228.
16. Joo, J.J., G.W. Reich, and J.T. Westfall, *Flexible Skin Development for Morphing Aircraft Applications via Topology Optimization.* Journal of Intelligent Material Systems and Structures, 2009. **20**(16): p. 1969-1985.
17. Bickel, B., et al., *Design and fabrication of materials with desired deformation behavior.* ACM Transactions on Graphics, 2010. **29**(4).
18. Lin, C.Y., et al., *Structural and mechanical evaluations of a topology optimized titanium interbody fusion cage fabricated by selective laser melting process.* J Biomed Mater Res A, 2007. **83**(2): p. 272-9.
19. Chen, Y., S. Zhou, and Q. Li, *Microstructure design of biodegradable scaffold and its effect on tissue regeneration.* Biomaterials, 2011. **32**(22): p. 5003-14.
20. Gorguluarslan, R.M., et al., *An improved lattice structure design optimization framework considering additive manufacturing constraints.* Rapid Prototyping Journal, 2017. **23**(2): p. 305-319.

21. Ma, Z.D., et al., *Experimental validation and prototyping of optimum designs obtained from topology optimization.* Structural and Multidisciplinary Optimization, 2006. **31**(5): p. 333-343.
22. Wang, B., et al., *Mechanical behavior of the sandwich structures with carbon fiber-reinforced pyramidal lattice truss core.* Materials & Design (1980-2015), 2010. **31**(5): p. 2659-2663.
23. Schramm, U. and M. Zhou, *Recent developments in the commercial implementation of topology optimization*. 2006. p. 239-248.
24. Ponginan, R., *Practical Aspects of Structural Optimization 3rd Edition*. 2018: Altair University.
25. Kim, N.H. and B.V. Sankar, *Introduction to Finite Element Analysis and Design*. 2008: Wiley.
26. Beer, F.P., *Mechanics of materials*. 5th ed. 2009, New York: McGraw-Hill Higher Education. xix, 790 p.

Appendix A. Building Block Library

σ_x	0				
σ_y \ σ_{xy}	−3	−1.5	0	1.5	3
4	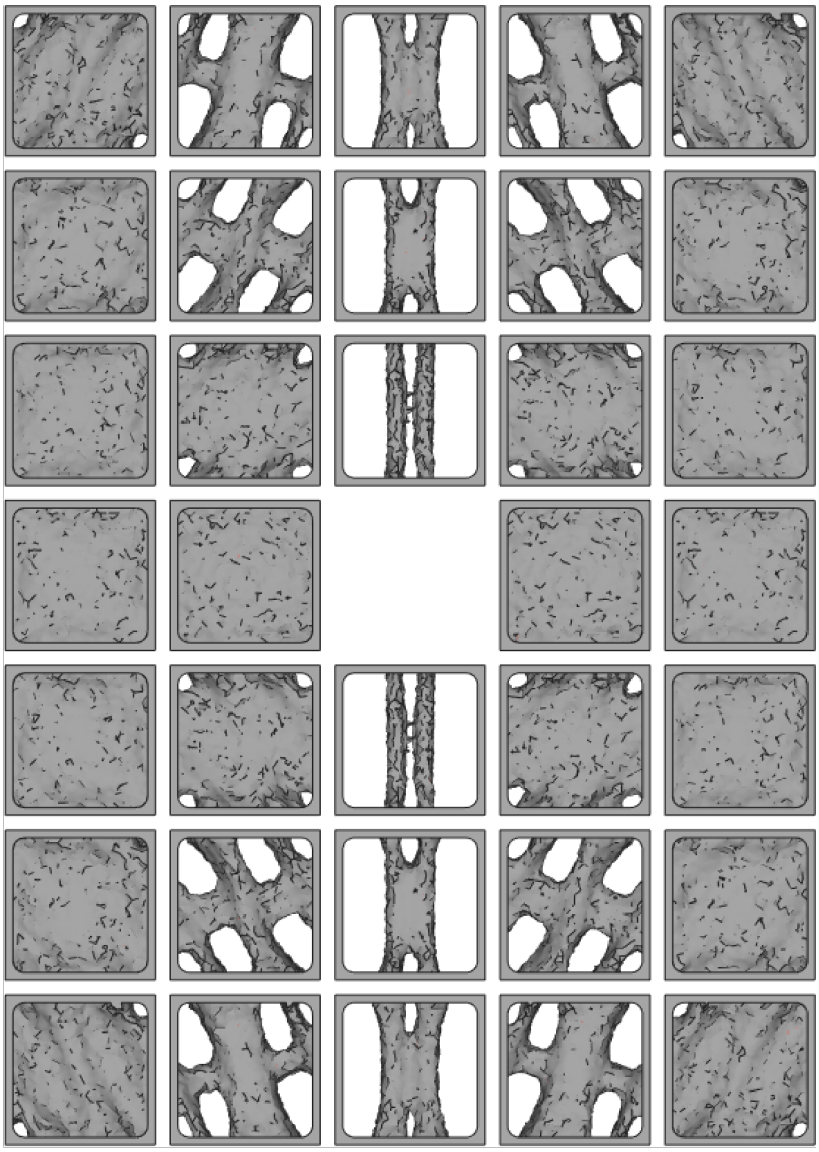				
2					
1					
0					
-1					
-2					
-4					

σ_x	−2				
σ_y \ σ_{xy}	−3	−1.5	0	1.5	3
4	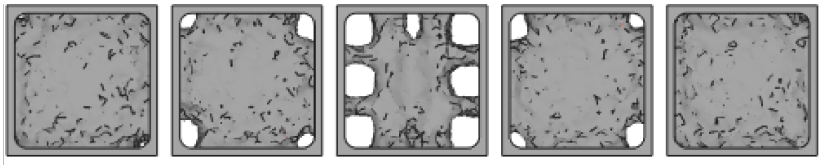				
2	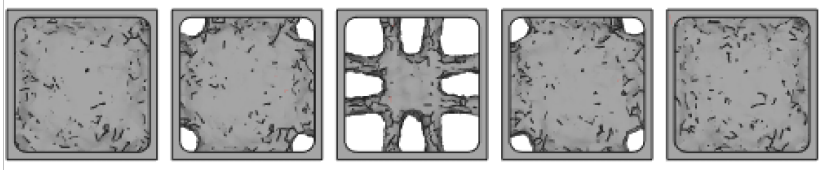				
1	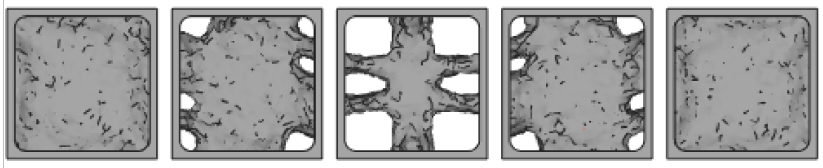				
0	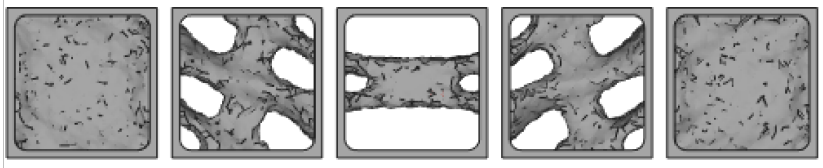				
-1					
-2	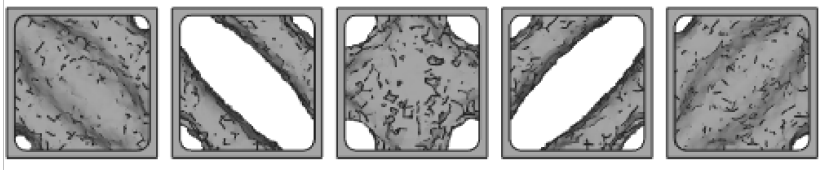				
-4	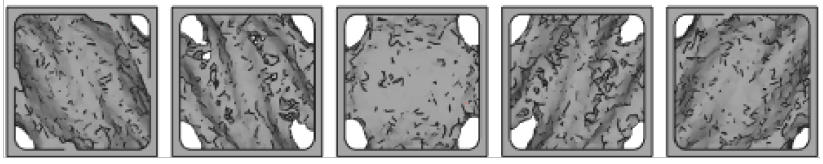				

σ_x	−4				
σ_y \ σ_{xy}	−3	−1.5	0	1.5	3
4	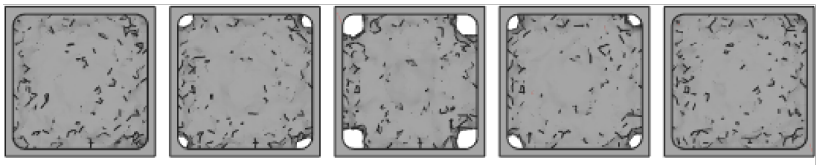				
2	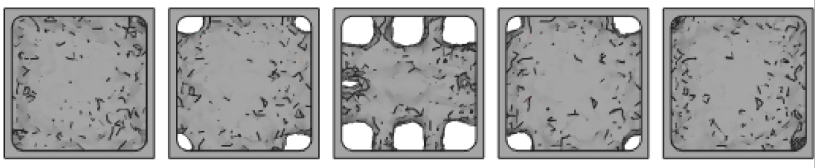				
1	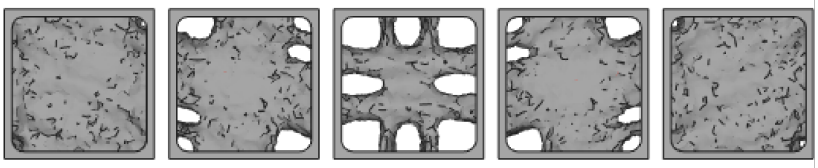				
0	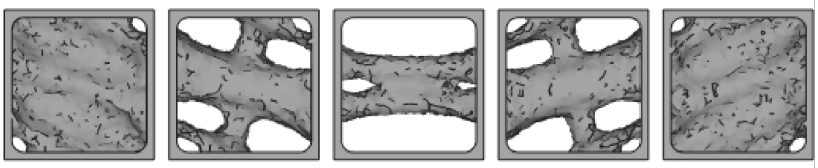				
-1	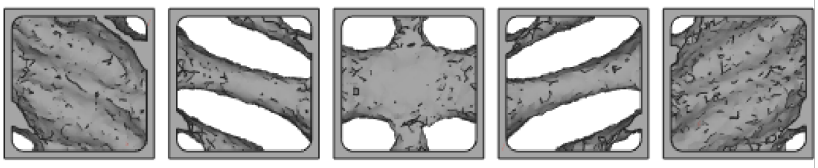				
-2	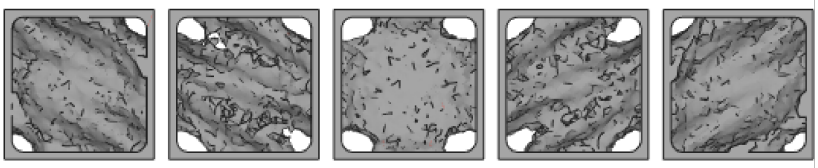				
-4	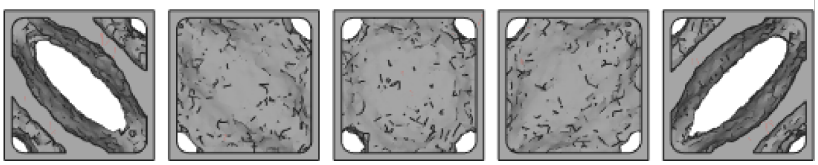				

σ_x	−8				
σ_y \ σ_{xy}	−3	−1.5	0	1.5	3
4	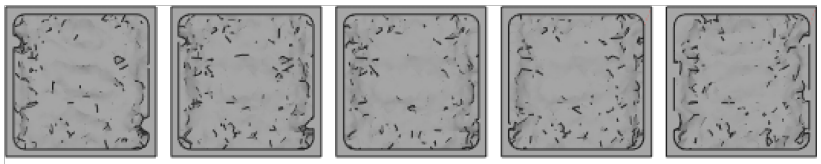				
2	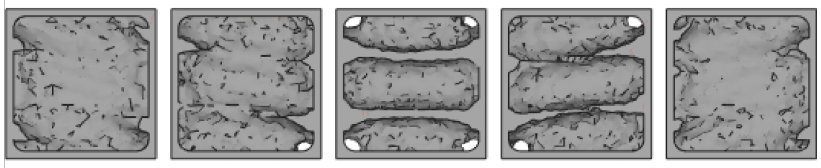				
1	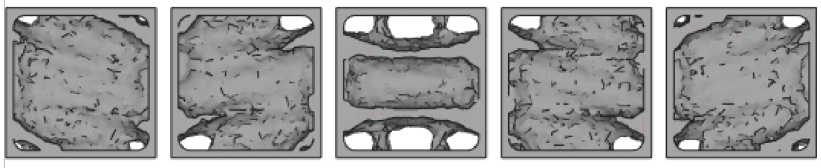				
0	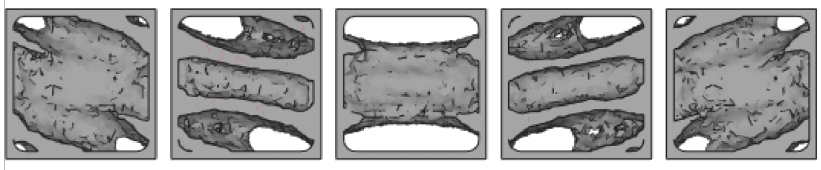				
-1	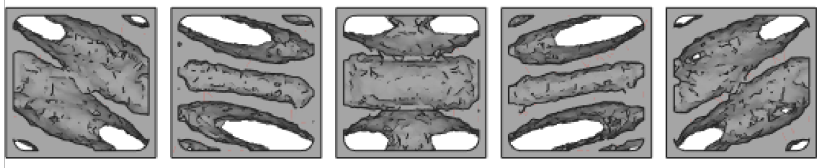				
-2	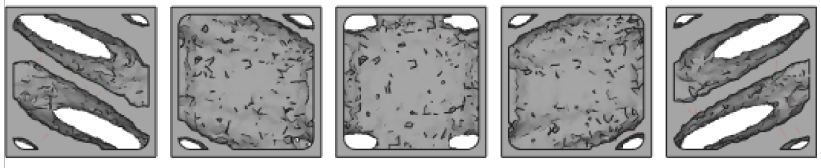				
-4	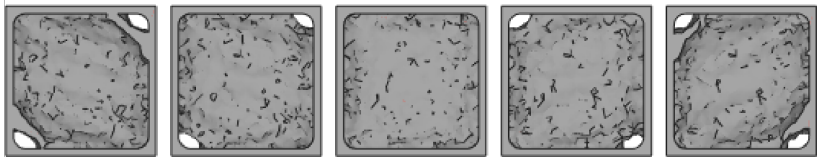				

σ_x	2				
σ_y \ σ_{xy}	−3	−1.5	0	1.5	3
4	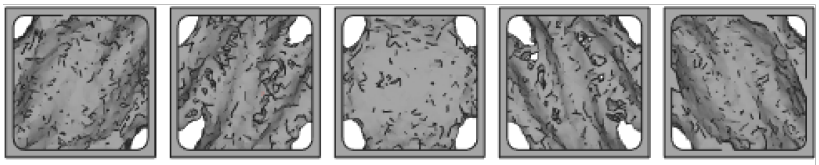				
2	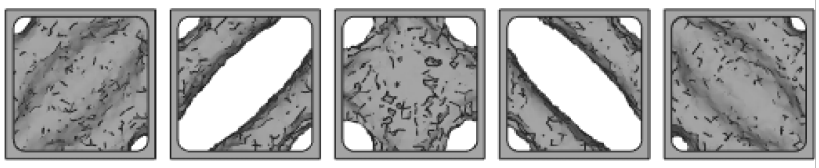				
1					
0	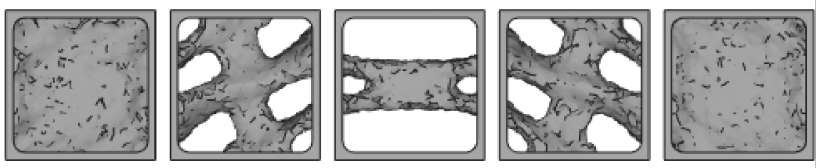				
-1	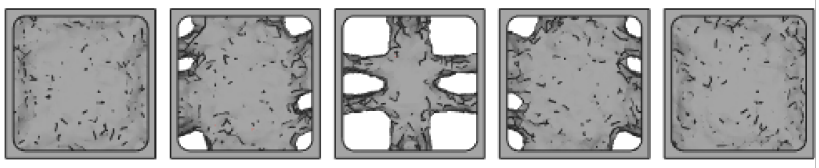				
-2	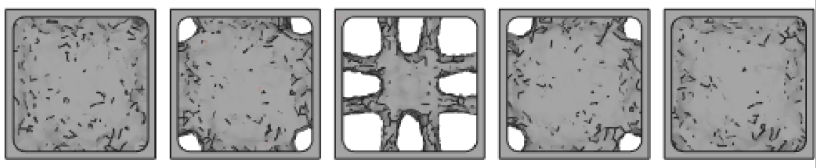				
-4	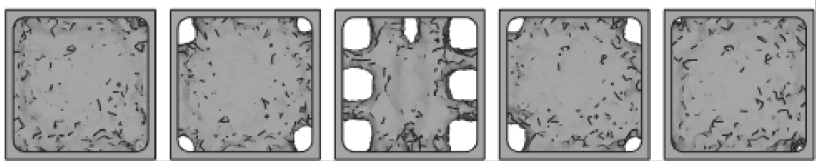				

σ_x	4				
σ_y \ σ_{xy}	−3	−1.5	0	1.5	3
4	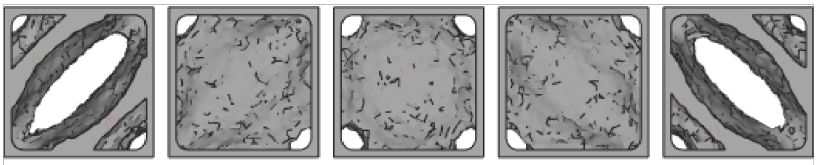				
2	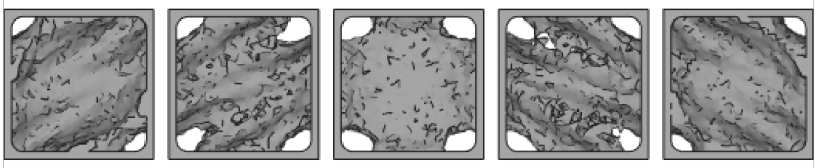				
1	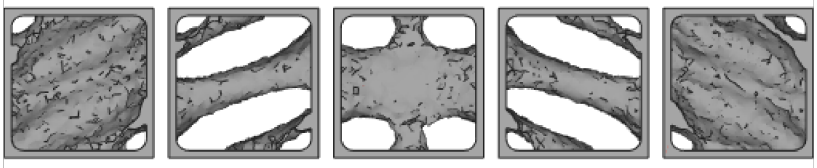				
0	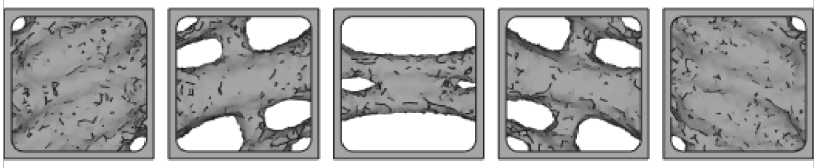				
-1	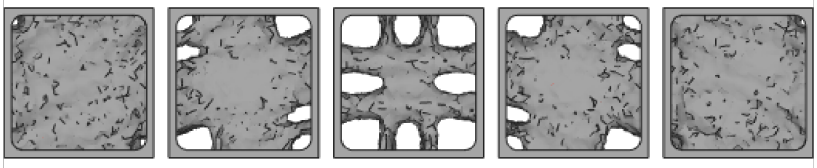				
-2	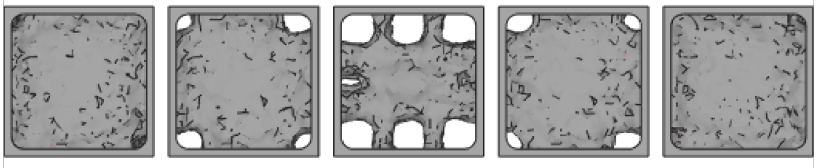				
-4	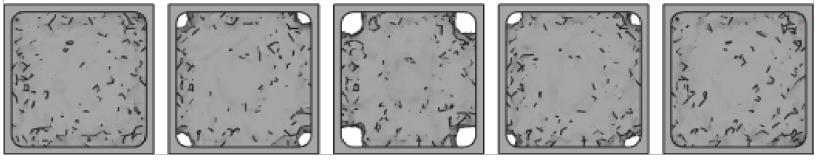				

σ_x	8				
σ_y \ σ_{xy}	-3	-1.5	0	1.5	3
4	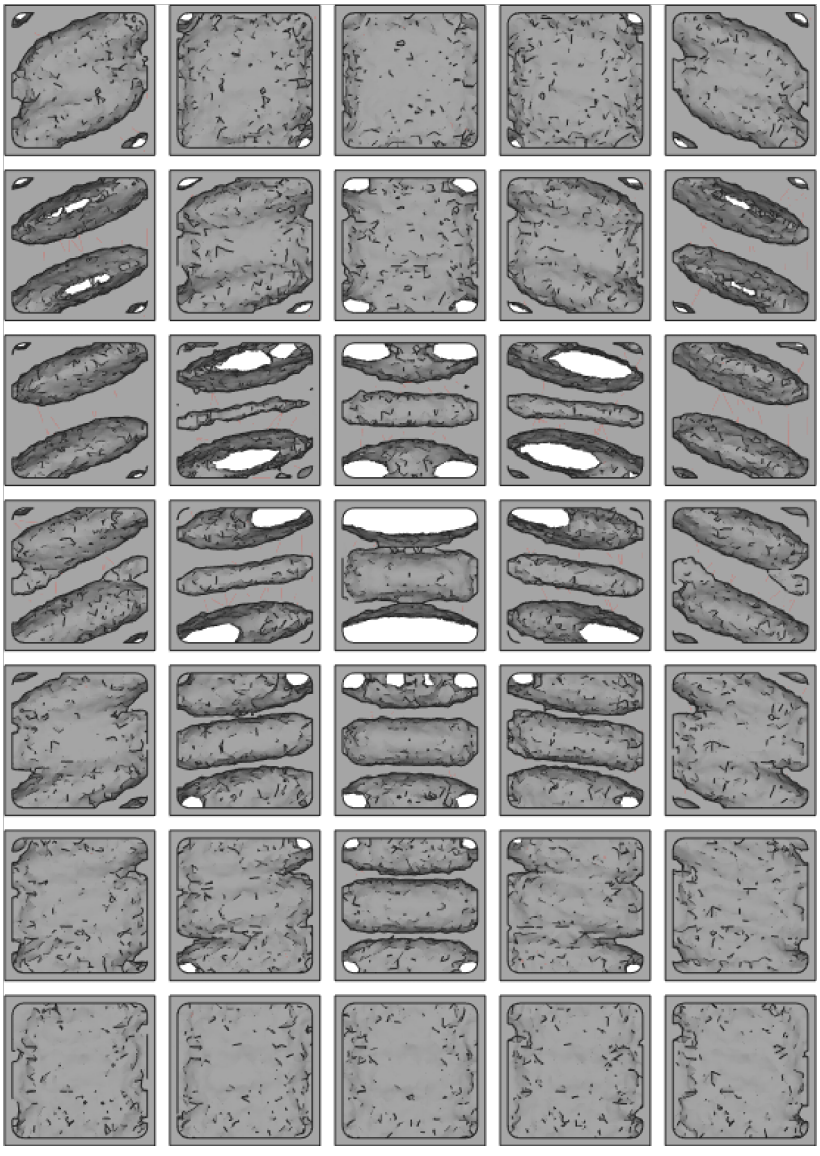				
2					
1					
0					
-1					
-2					
-4					

Appendix B. Python Script for Load Case .csv Files Generation

In the loads panel in the inspire software, load cases export can be exported to get the load cases in .csv format. The details of the load cases can be modified by substituting the values in the file.

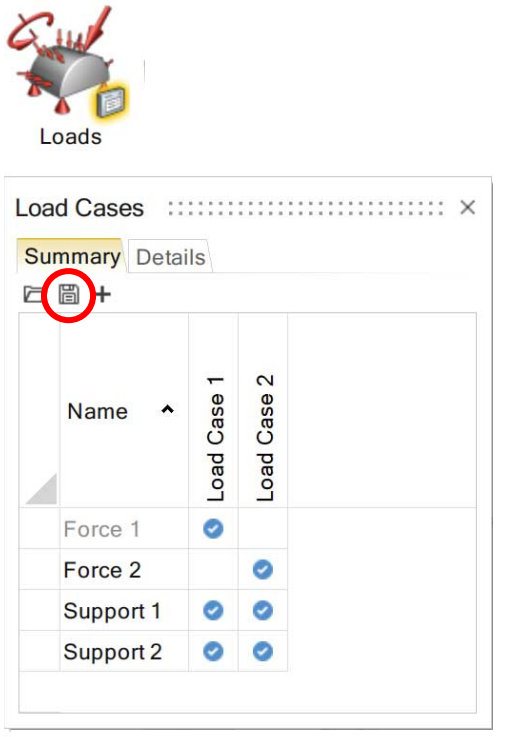

Following python code was executed to generate the entire stress conditions, substitute the values in each load case and generate CSV file for the whole set of load cases.

```
 import csv
 import pandas as pd
 import copy
 df_frame = pd.read_csv('LoadTableExport.csv', header=5)
 support = df_frame.drop([8,9,10,11,12,13,14,15],axis = 0)
 P_x = [8, 4, 2, 0, -2, -4, -8]
 P_z = [4, 2, 1, 0, -1, -2, -4]
 P_xz = [3, 1.5, 0, -1.5, -3]
 tensor = []
 for x in P_x:
     for z in P_z:
         for xz in P_xz:
             tensor.append([x,z,xz])
 case_code = []
 for t in tensor:
     case_code.append(str(t[0])+'_'+str(t[1])+'_'+str(t[2]))
 df_default = copy.deepcopy(df_frame)
 # Leave only default supports
 df_frame = pd.concat([df_frame,
df_default.drop([8,9,10,11,12,13,14,15],axis=0)])
 for t in tensor:
     if t[0] > 0:
         df_default.iloc[8,8]=-1
         df_default.iloc[9,8]=1
     else:
         df_default.iloc[8,8]=1
         df_default.iloc[9,8]=-1
     if t[1] > 0:
         df_default.iloc[10,9]=1
         df_default.iloc[11,9]=-1
     else:
         df_default.iloc[10,9]=-1
         df_default.iloc[11,9]=1
     if t[2] > 0:
         df_default.iloc[12,9]=-1
         df_default.iloc[13,9]=1
         df_default.iloc[14,8]=1
         df_default.iloc[15,8]=-1
     else:
         df_default.iloc[12,9]=1
         df_default.iloc[13,9]=-1
         df_default.iloc[14,8]=-1
         df_default.iloc[15,8]=1

     df_default.iloc[0:16,0] = 'Load_Case_' +
str(t[0])+'_'+str(t[1])+'_'+str(t[2])
     df_default.iloc[8,1]='Normal_Left_'+str(t[0])
     df_default.iloc[9,1]='Normal_Right_'+str(t[0])
     df_default.iloc[8:10,6]=abs(t[0])
     df_default.iloc[10,1]='Normal_Top_'+str(t[1])
     df_default.iloc[11,1]='Normal_Bottom_'+str(t[1])
     df_default.iloc[10:12,6]=abs(t[1])
     df_default.iloc[12,1]='Shear_Left_'+str(t[2])
     df_default.iloc[13,1]='Shear_Right_'+str(t[2])
     df_default.iloc[14,1]='Shear_Top_'+str(t[2])
     df_default.iloc[15,1]='Shear_Bot_'+str(t[2])
```

```
    df_default.iloc[12:16,6]=abs(t[2])
    df_frame = pd.concat([df_frame, df_default[8:16]])
df_result=df_frame[16:]
df_result.to_csv('Extra_Cases1.csv', index = False)
```

Appendix C. Python Script for .odb (Output Database) File Access

The ABAQUS Command prompt provides python scripting interface that can be started with the command *abaqus python* as shown in below figure. In the prompt, users can use the odbAccess library to access the output database file (.odb file) and obtain structural analysis result from ABAQUS.

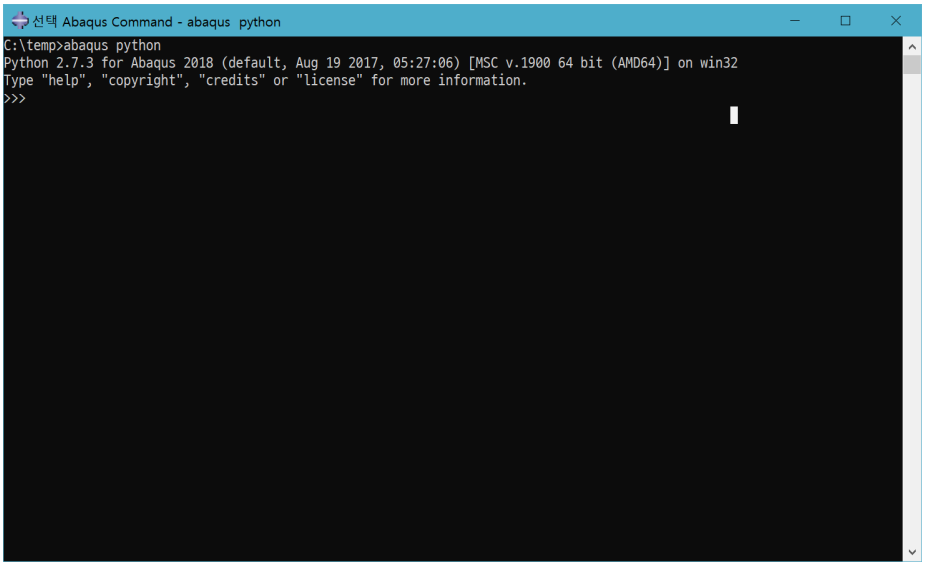

The following python code was written to obtain the stress distribution data from the elements and save them into a .csv file.

```
from odbAccess import *
import csv
import time

start_time = time.time()
directory = '..\\0_Initial_Analysis'
name = 'Bridge'

li = []

odb = openOdb(path=directory + '\\' + name + '.odb')
count = 0
Frames = odb.steps['Step-1'].frames
Values = Frames[-1].fieldOutputs['S'].values
for value in Values:
    li.append(value.data)

with open(directory + '\\' + name  + '.csv', 'wb') as csvfile:
    datawriter = csv.writer(csvfile, delimiter=',',
                            quotechar='|', quoting=csv.QUOTE_MINIMAL)
    datawriter.writerow(['X Normal', 'Y Normal', 'Z Normal', 'XY
Shear', 'YZ Shear', 'ZX Shear'])
    for f in li:
        datawriter.writerow(f)
```

Appendix D. MATLAB Code for Building Block Stacking Phase

The MATLAB code that regulates the building block stacking phase is presented below.

```
tic;
clear all; clc;

%% Variables setting

% 1.Geometry grid section variables
% The geometry should be ractangle with the origin on 'box_min_cord'
% (X,Y,Z length = 'box_size')
% The geometry will be grided with 'mesh_size' cubes.
% Cell size of each cell should be set as 'cell_size' (for scaling)

grid_size=20; %in mm
cell_size=100;
box_min_cord=[0 0 0];
box_size=[220 20 40];

% 2. Structure generation section variables
job_file_path = '..\0_Initial_Analysis\';
job_name = 'Bridge'

% 3. Assembly write section variables
stl_files_path = [pwd '\cad_files\'];

%% Geometry grid Section

name='Bridge';
filename=[job_file_path name '.stl'];

min = 0.00001;
xgrid1=[box_min_cord(1)+min:grid_size:box_min_cord(1)+box_size(1)+min]
;
ygrid1=[box_min_cord(2)+min:grid_size:box_min_cord(2)+box_size(2)+min]
;
zgrid1=[box_min_cord(3)+min:grid_size:box_min_cord(3)+box_size(3)+min]
;

xgrid2=linspace(box_min_cord(1)+grid_size/2,
box_min_cord(1)+box_size(1)-grid_size/2, box_size(1)/grid_size);
ygrid2=linspace(box_min_cord(2)+grid_size/2,
box_min_cord(2)+box_size(2)-grid_size/2, box_size(2)/grid_size);
zgrid2=linspace(box_min_cord(3)+grid_size/2,
box_min_cord(3)+box_size(3)-grid_size/2, box_size(3)/grid_size);

display('Grided')
%% Structure generation section

% Reading element stress data
display('Read element stress data')
stress_data = csvread([job_file_path job_name '.csv'],1,0);

% Reading input data (for element-node coordinate data)
[nodes, elements] = read_inp_3D([job_file_path job_name '.inp']);
```

```
 display('Read geometry data from inp')

 [structure_code stress_cell]=
eval_structure(xgrid1,ygrid1,zgrid1,nodes,elements,stress_data);
 display('Structure_code generated')

 %% Assembly section
 output_name = '..\3_ABAQUS_input_generation\comp_upsidedown.stl';
 assembly_write(output_name, stl_files_path, structure_code,xgrid2,
ygrid2, zgrid2, grid_size, cell_size);
 toc;
```

Acknowledgement

I want to express sincere gratitude to the people who helped me writing this thesis. It would not have been possible to complete the master's program and thesis if there were no guidance and support of the people.

First of all, I appreciate the guidance and help of my advisor, Prof. Namhun Kim. He always has been a great supporter and teacher. He encouraged me to think deep and find an original solution and suggested great ideas when there are obstacles. Also, I appreciate committee members of my thesis, Prof. Juwhan Oh and Prof. Duck Young Kim. They gave me insightful advice on the thesis.

Thanks to my colleagues, I could learn so much and endure hard times during the master's degree program. Dr. Eunju Park and Dr. Moise Busogi gave me detailed guidance of the research approach and thesis writing. My senior colleagues, Sangho Ha and Jungsik Kim, helped me get through hard times by sharing their experiences. During many research projects and thesis writing process, Eunseo, Munyoung and I have overcome difficult moments together. Encountering new things, discussing and solving problems together, we gained invaluable experiences and made good memories. I am happy that I made these good friends during my graduate program. Haekwon read through my thesis in detail and helped me proofread the thesis as if it is his thesis. I appreciate all the help I received from my colleagues.

At last, I appreciate my mother, father and sister. Without their limitless and love and support, I could not be able to get through all of it.